# CURRENT STATUS OF PRECISION PDT TREATMENT PLANNING: PHYSICAL AND BIOLOGICAL CONSIDERATIONS

**Lothar Lilge**

**Princess Margaret Cancer Centre/University Health Network**

**Department of Medical Biophysics/ University of Toronto**

**Canada**

# Collaborators

**Clinical:**

**Girish Kulkani, Michael Jewett, Kazuhiro Yasufuku, Marcelo Cypel, Khaled Ramadan,** UHN, Canada

**Collaborators:**

**Brian Wilson, Robert Weersink**

UHN, Canada

**Sherri McFarland** UTA, Texas

**Computer Sciences:**

**Vaughn Betz, Jeff Cassidy,** Fynn Schwiegelshohn, **Abdul-Amir Yassine, Tanner Young-Schultz, Yasmin Afsharnezhad, Helen Dai, Zihao Chen, Shengxiang Ji, Shuran Wang** University of Toronto, Canada

**Students:**

**Carl Fisher, Daniel Molehuis, Angelica Manalac, Chris McFadden, William Lo, Yiwen Xu, Tina Saeidi, Wania Khan**

**Industrial:**

**Savo Lazic, Pavel Kaspler, Mark Roufaiel, Arkady Mandel, Wayne Embree, Leonid Vesselov, Roger White** Theralase Inc. Toronto, Canada

**Dirk Huettenberger** Synverdis GMBH, Heidelberg, Germany

# Photodynamic Therapy

- First clinical approval 1993 (Bladder Cancer)
- 16 K publication 1993-now containing ‘clinical’ or ‘patient’ as keywords
- 70 ongoing clinical trials in oncology (superficial ~45 vs. interstitial ~20)
- Approval based on administered Photosensitizer [mg/kg] and delivered optical energy [J $cm^{-2}$], [J $cm^{-1}$], or [J]
- Benefit of repeat therapies - particular for immune response.

## Trans Surface Accessible Illumination

- Large surface area illumination
- Photon density gradient given by $1/\mu_{eff}$
  - Possible Photosensitizer gradient
- Lack of eloquent structures
  - Exception Bladder
- Good healing

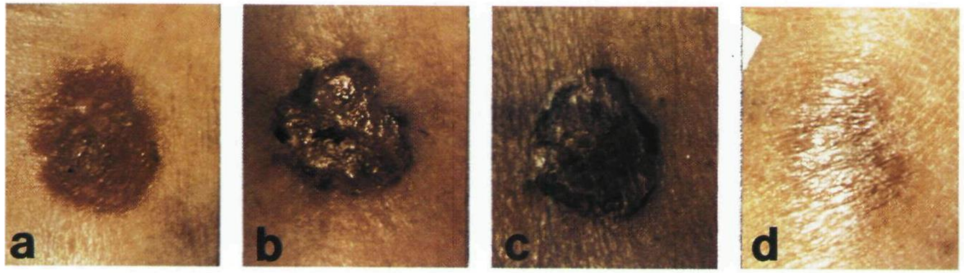


- Curative therapy – First line therapy

## Deep Seated or Solid Target

- Source number volume dependent
- Photon density gradient given by $1/\pi r\ \mu_{eff}$ or $1/\pi r^2\ \mu_{eff}$
- Eloquent structures can be present
- Necrotic tissue removal
- Salvage therapy
  - Exception Prostate, GBM

# Interstitial Photodynamic Therapy
# Current Treatment planning concepts

- Drug dose  [mg/kg],  Energy delivered [J or J/cm or J/cm$^2$], heuristic Light source placement, spacing determined by tissue and PDT wavelength


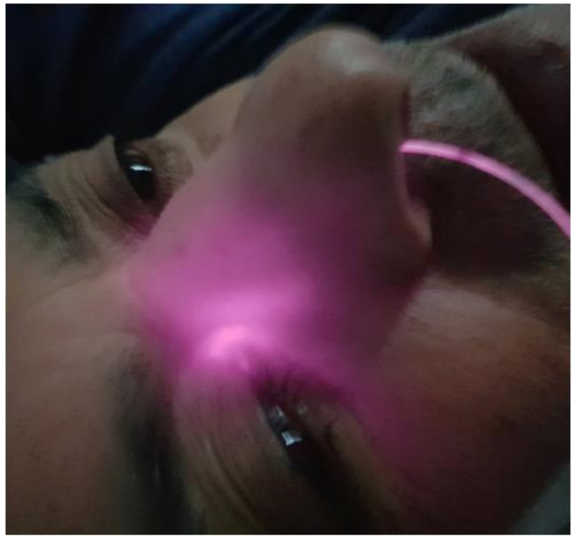
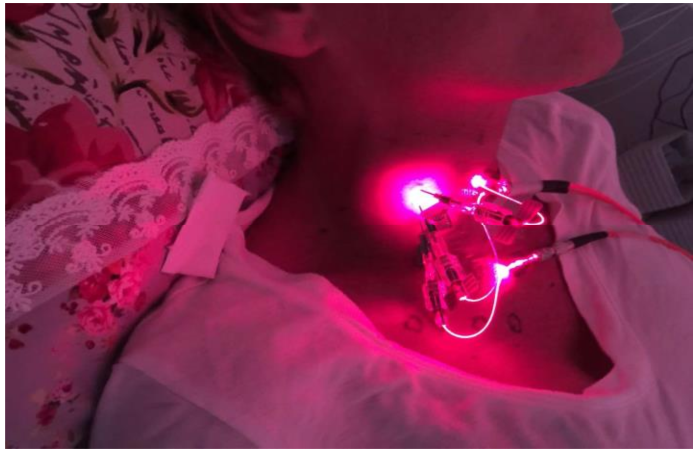
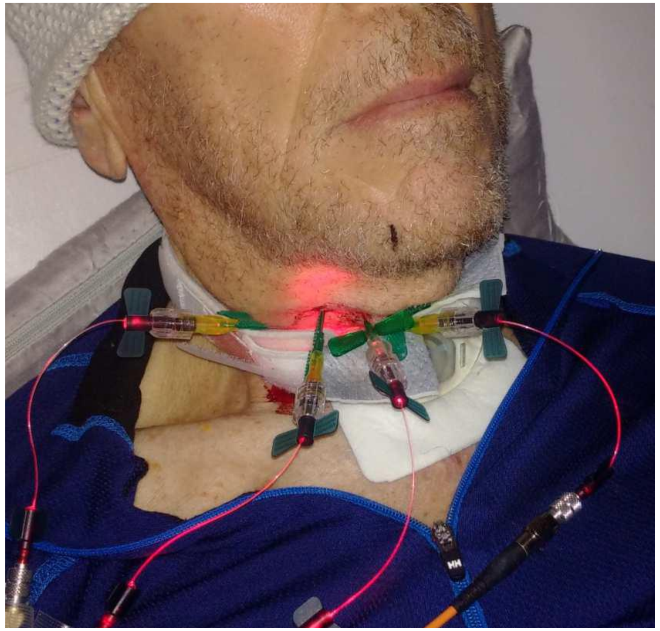

- Validating Light source placement, dose definition and progress monitoring.

# Example iPDT for Malignant Glioma

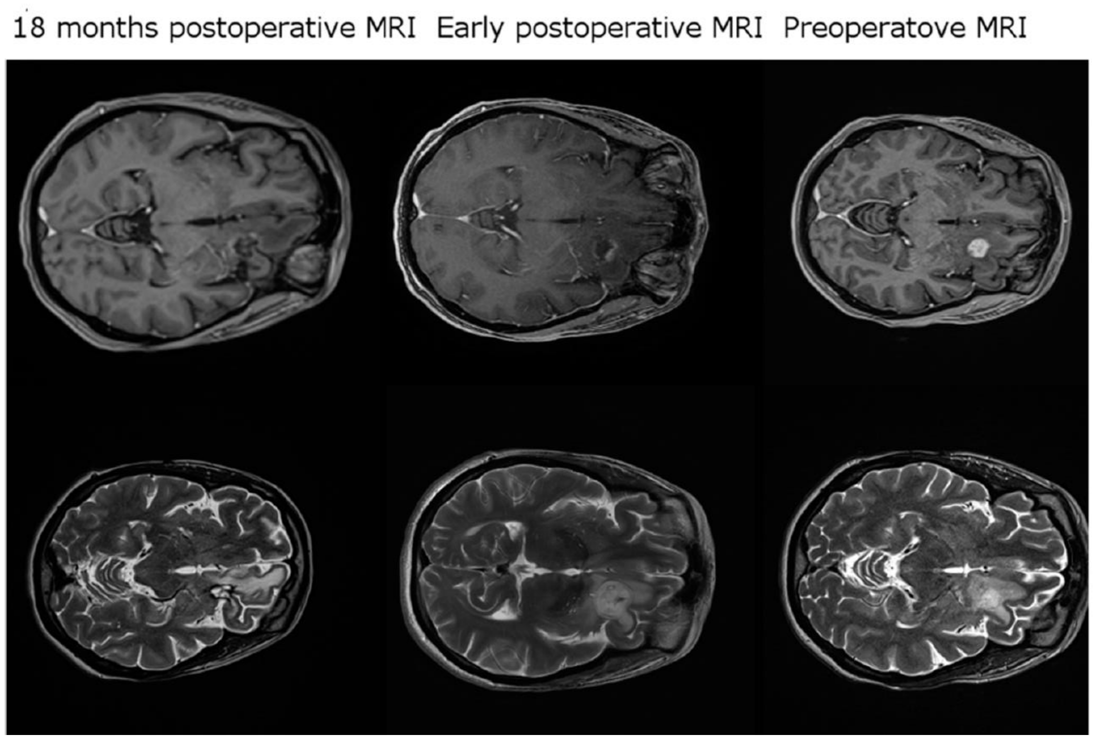


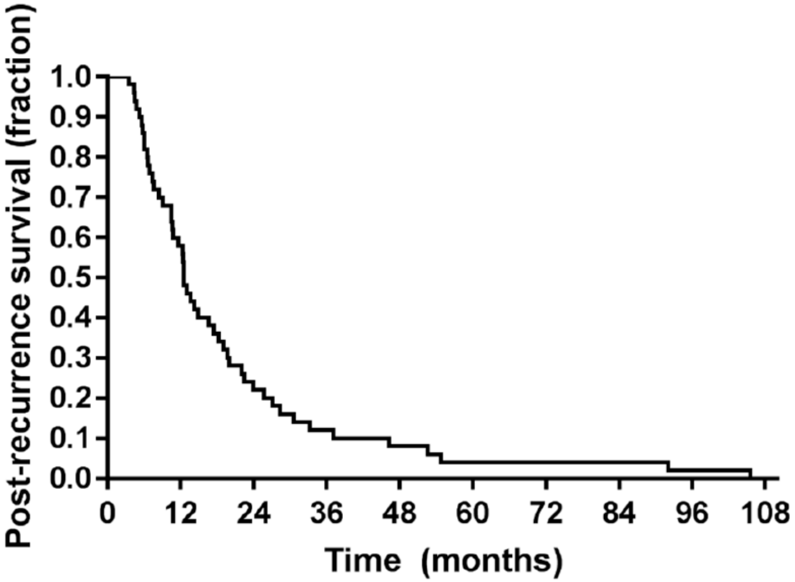


Lietke S et al. Interstitial Photodynamic Therapy Using 5-ALA for Malignant Glioma Recurrences, Cancers 2021, 13, 1767. https://doi.org/10.3390/cancers 13081767

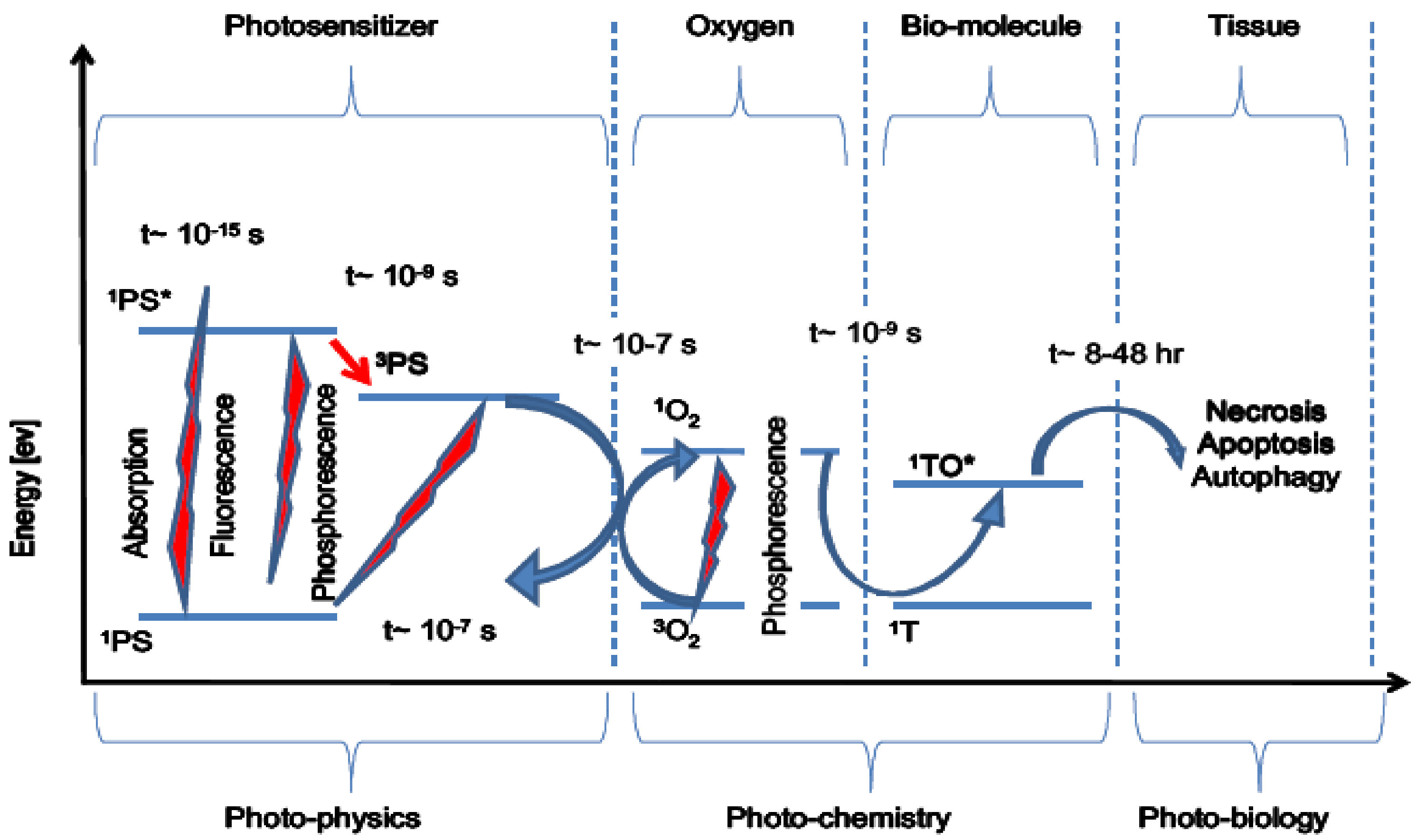


Monitoring

Planning

Photodynamic Therapy needs temporal and spatial overlap of Photosensitizer, Oxygen and Photons with appropriate quantum energy

# Light delivery Outer surface

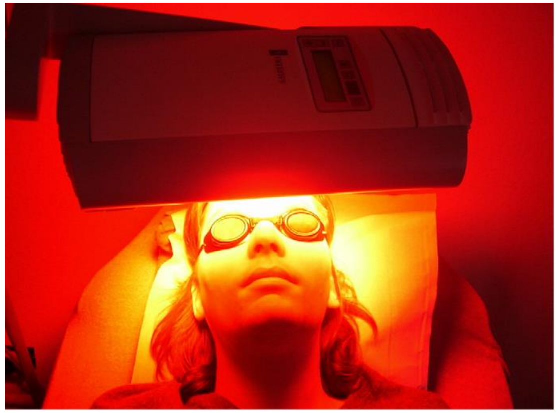

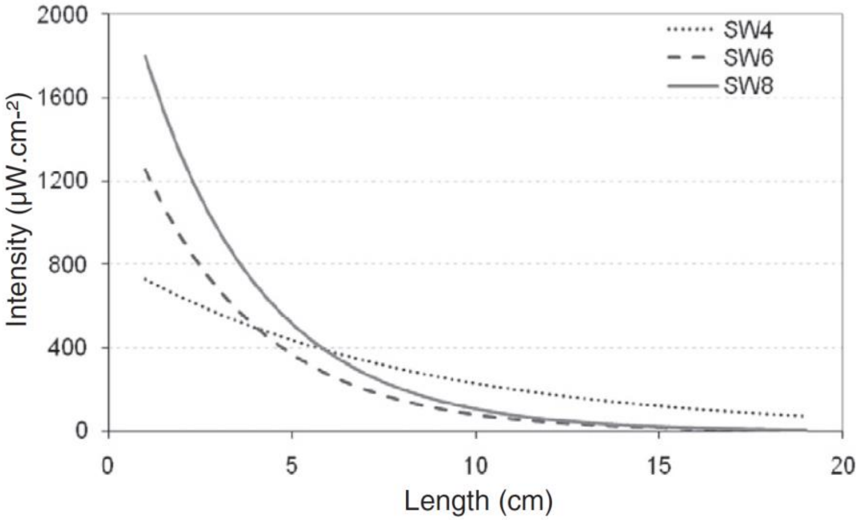


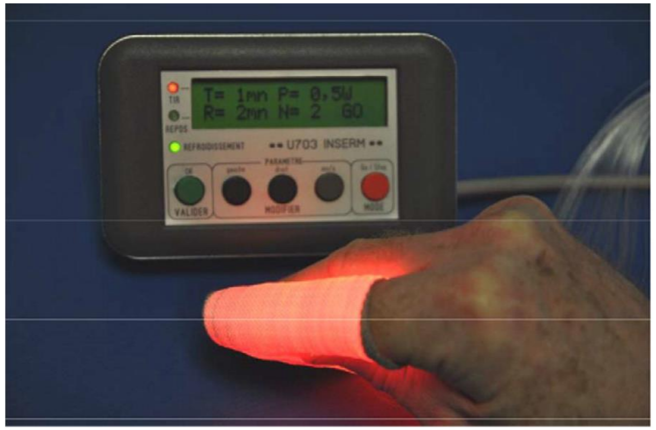

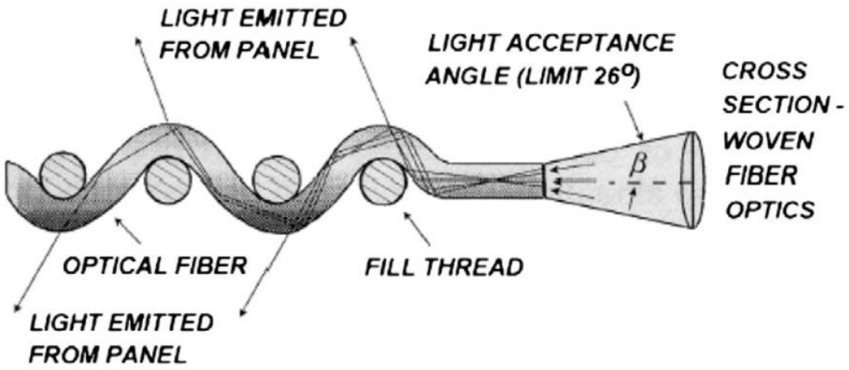


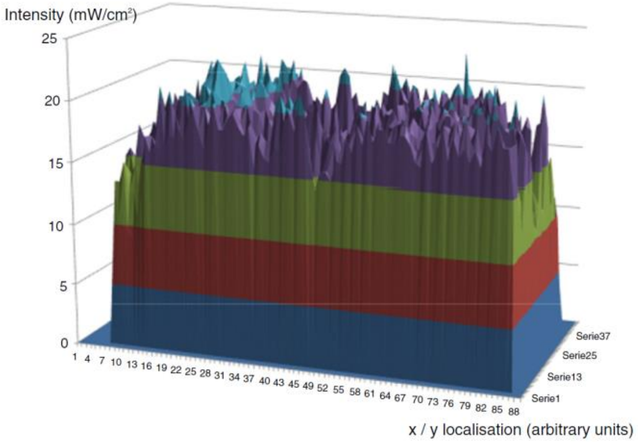


Cochrane C et al New design of textile light diffusers for photodynamic therapy Materials Science and Engineering C 33 (2013) 1170–1175

Mordon SR et al. Light emitting fabrics for PDT: technology and results of clinical studies. Proc. SPIE 11070, 110705L doi: 10.1117/12.2534874

# Surgical access allowing surface PDT applications

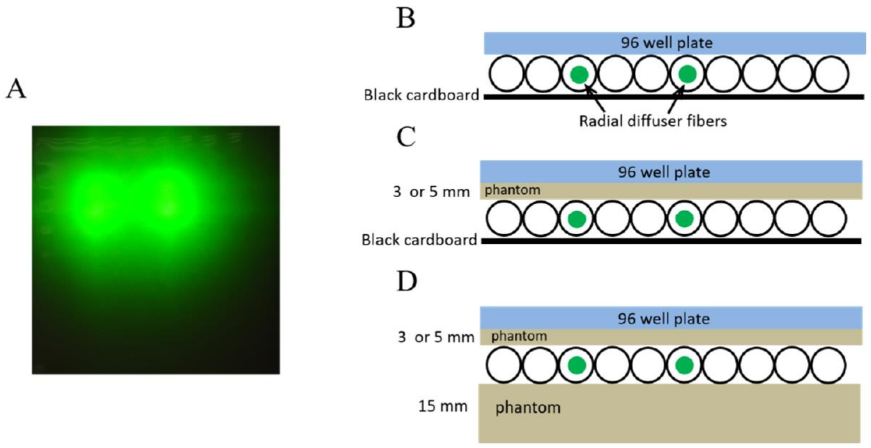


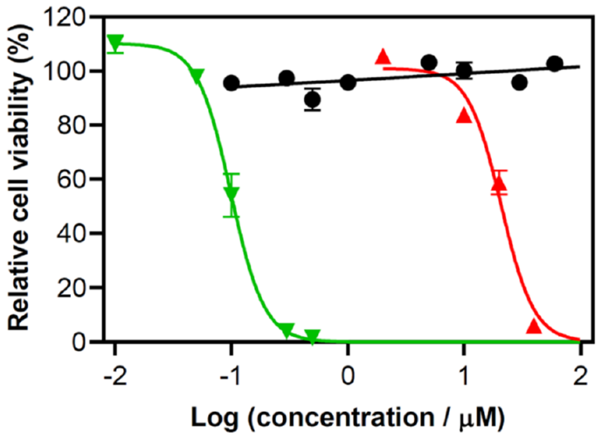


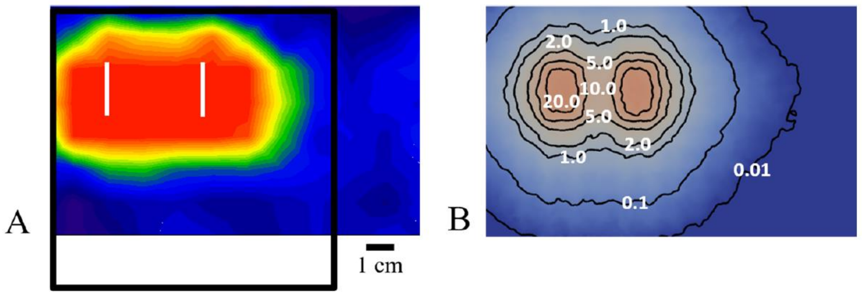


| Percent Viability (%) | Irradiance Range (mW/cm²) | Fluence Range (J/cm²) |
|---|---|---|
| 0 | >10 | >20 |
| 20 | 3 - 10 | 10 - 20 |
| 40 | 2 - 3 | 5 - 10 |
| 60 | 0.05 - 2 | 2 - 5 |
| 80 | 0.01 – 0.05 | 0.01 – 2 |
| 100 | <0.01 | <0.01 |

Chamberlain S et al. TLD1433-Mediated Photodynamic Therapy with an Optical Surface Applicator in the Treatment of Lung Cancer Cells In Vitro Pharmaceuticals 2020, 13, 137; doi:10.3390/ph13070137

# Fluence Dosimetry in Cavity

$$\phi_{dir} = \frac{S}{4\pi r^2} A(\theta),$$

$$\int_0^{\pi} A(\theta) d\Omega / 4\pi = 1$$

$$\phi_{sc} = \frac{4S}{A_s} \cdot R_d \cdot (1 + R_d(1-f) + R_d^2(1-f)^2 + \ldots) = \frac{4S}{A_s} \cdot \frac{R_d}{1 - R_d(1-f)},$$

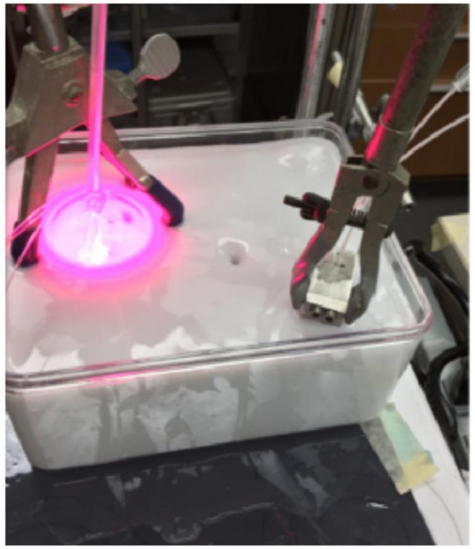

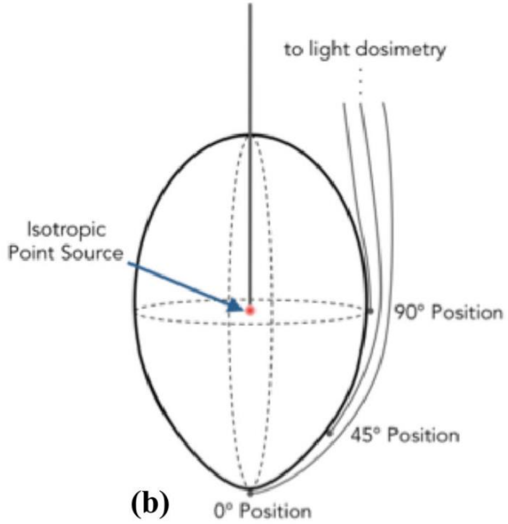


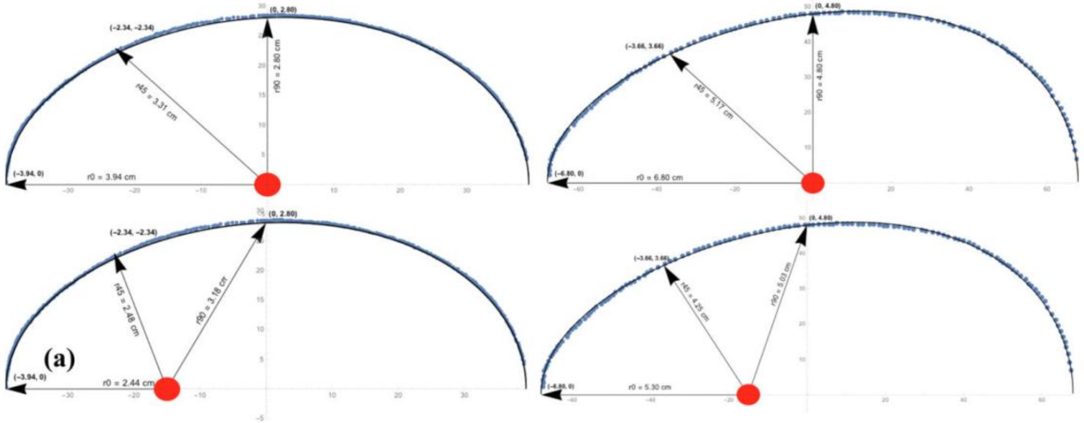


Zhu TC et al. Light Fluence Dosimetry in Lung-simulating Cavities Proc SPIE Int Soc Opt Eng. 2018 ; 10476: . doi:10.1117/12.2291355.

# Bladder Surface Irradiance homogeneity

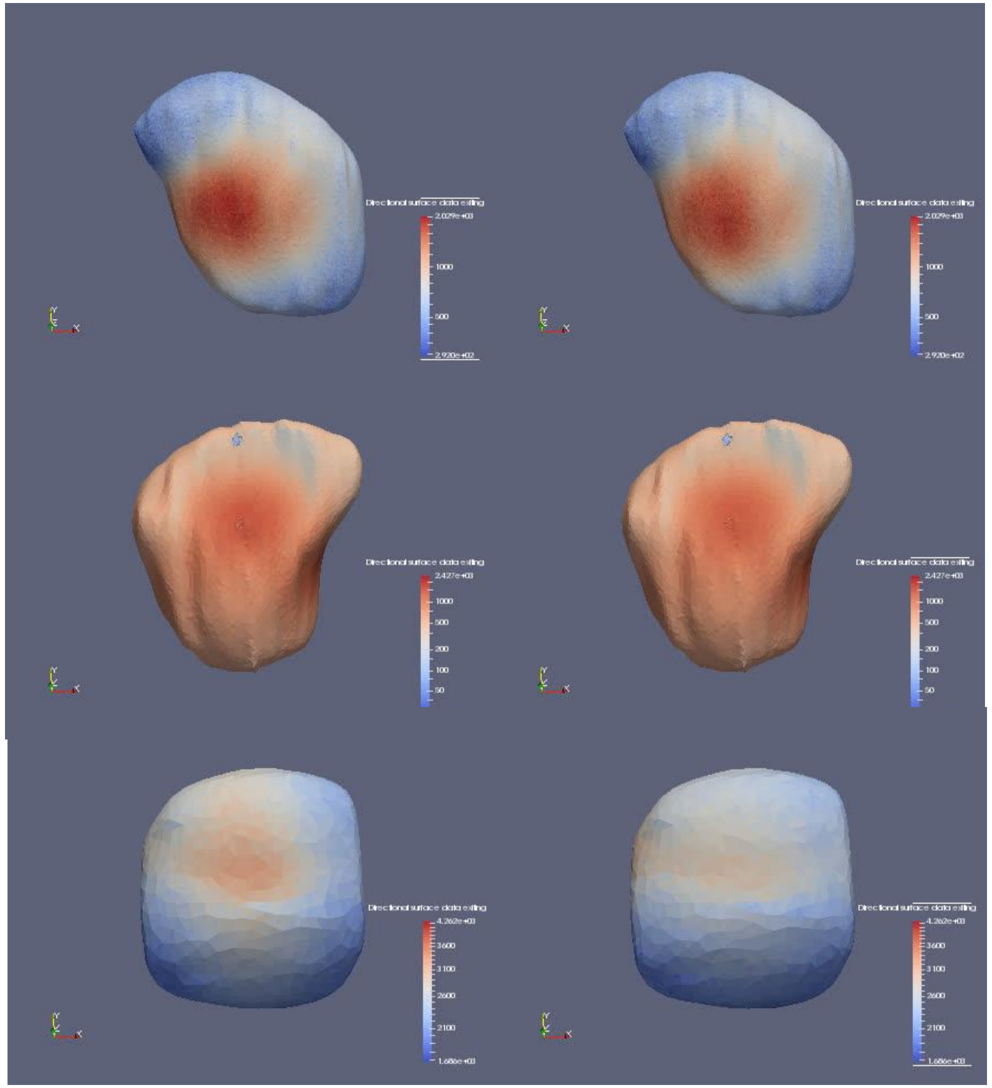

Surface area

173.6 cm²

190.9 cm²

48.4 cm²

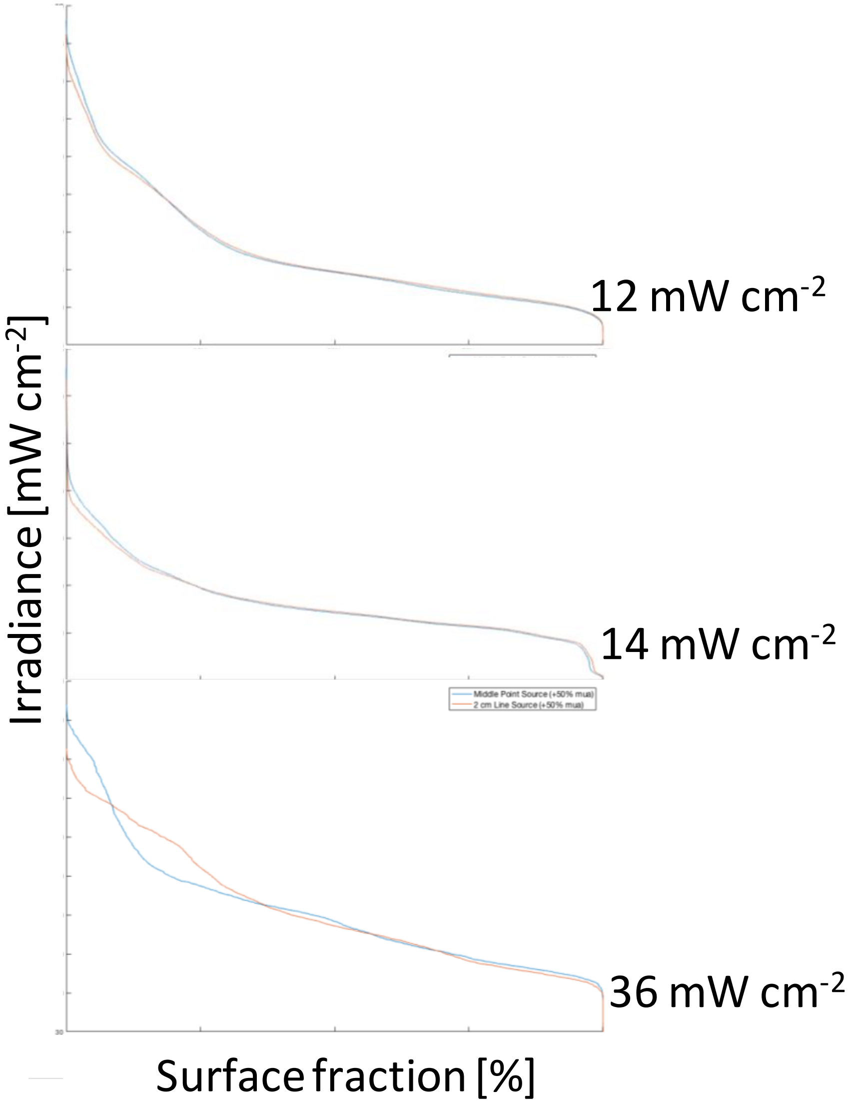


Lilge L, Wu J, Xu Y, et al. Minimal required PDT light dosimetry for Non-Muscle Invasive Bladder cancer. Journal of Biomedical Optics, 25(6), 068001 , (2020)

# Photosensitizer based Surface Dosimetry

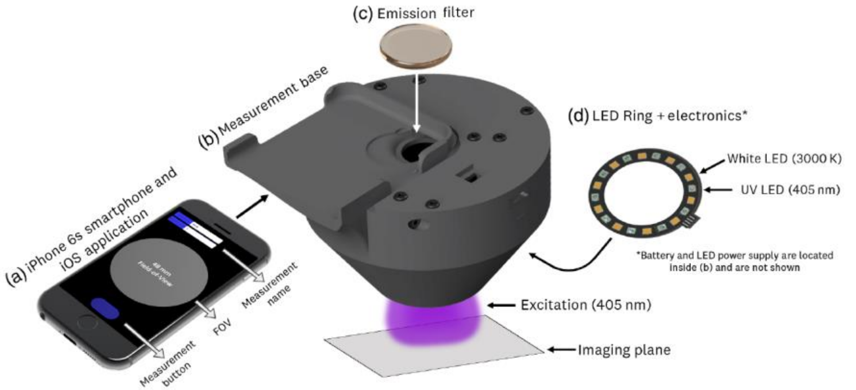


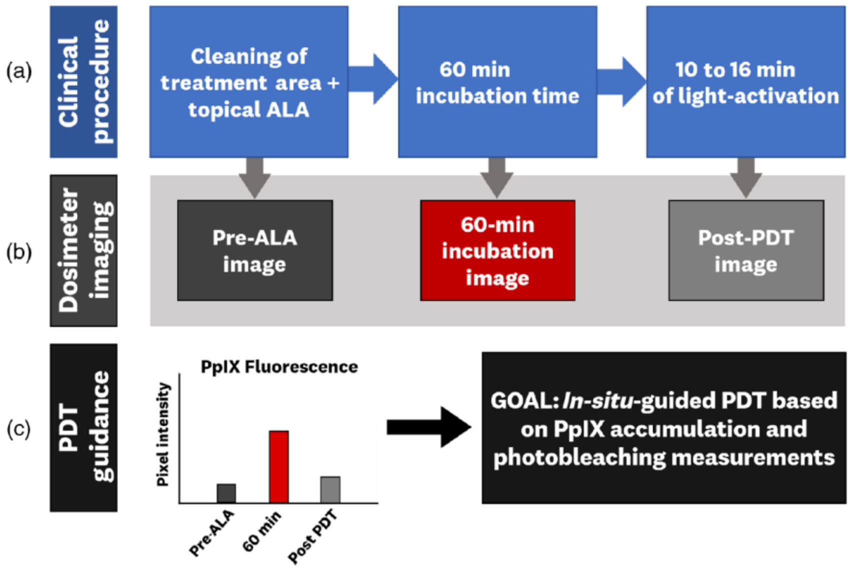


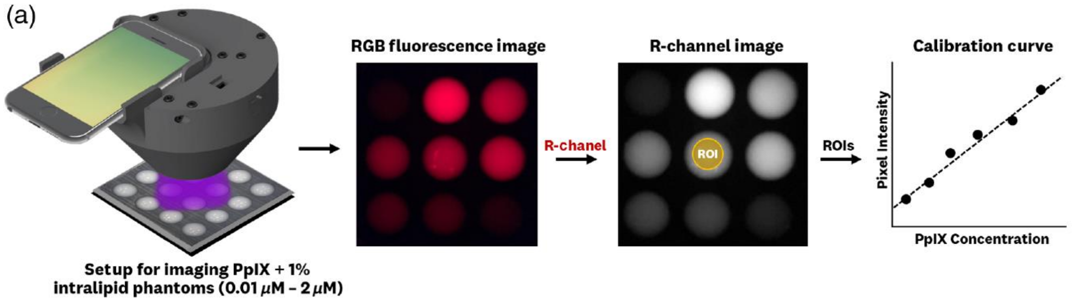


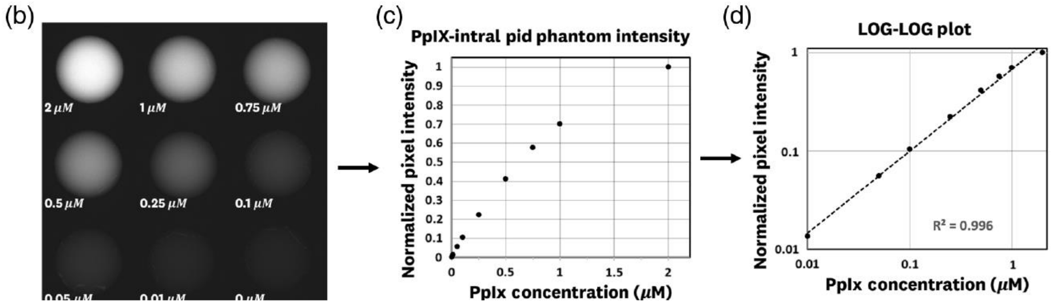


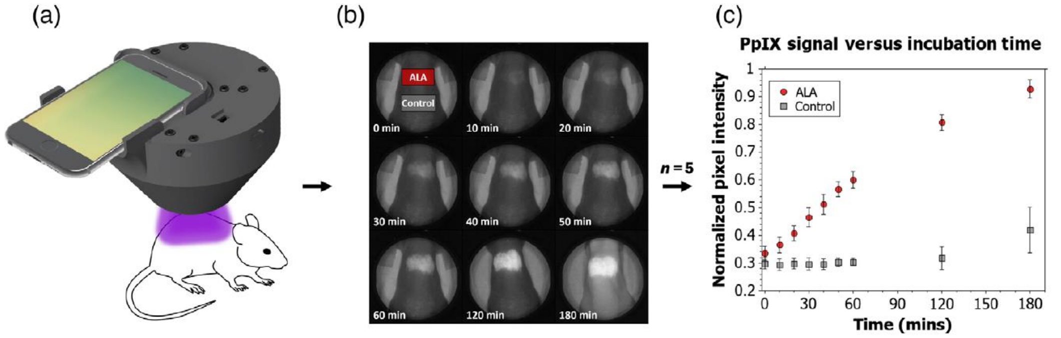


Ruiz AJ et al Smartphone fluorescence imager for quantitative dosimetry of protoporphyrin-IX-based photodynamic therapy in skin J. Biomed. Opt. 25(6), 063802 (2019), doi: 10.1117/1.JBO.25.6.063802.

# iPDT treatment plan based on Templates and Clinical Imaging

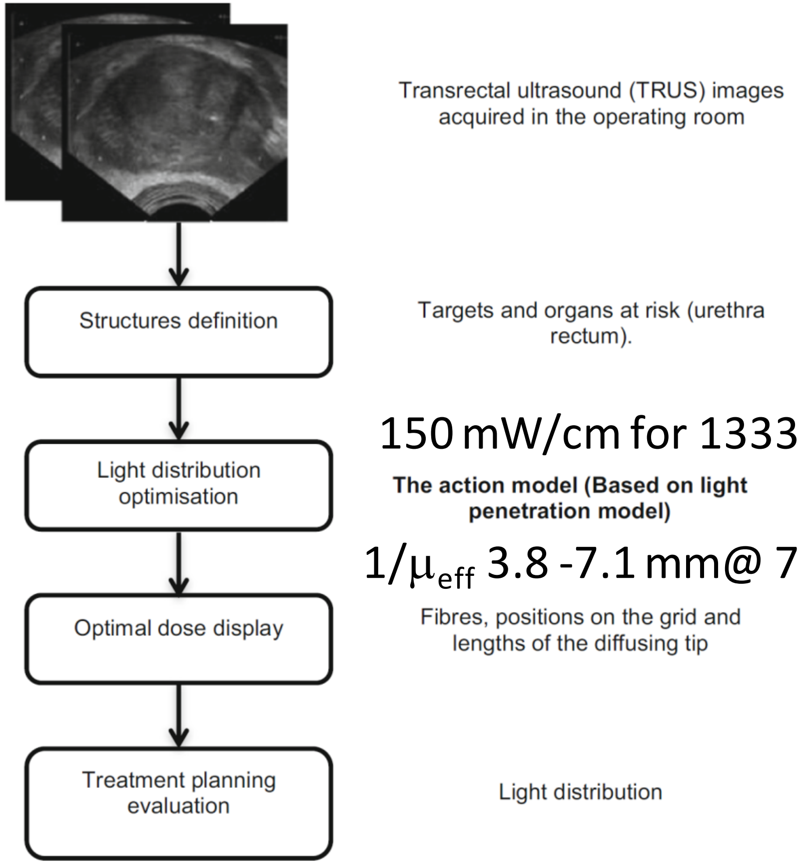


150 mW/cm for 1333 sec

$1/\mu_{eff}$ 3.8 -7.1 mm@ 753 nm

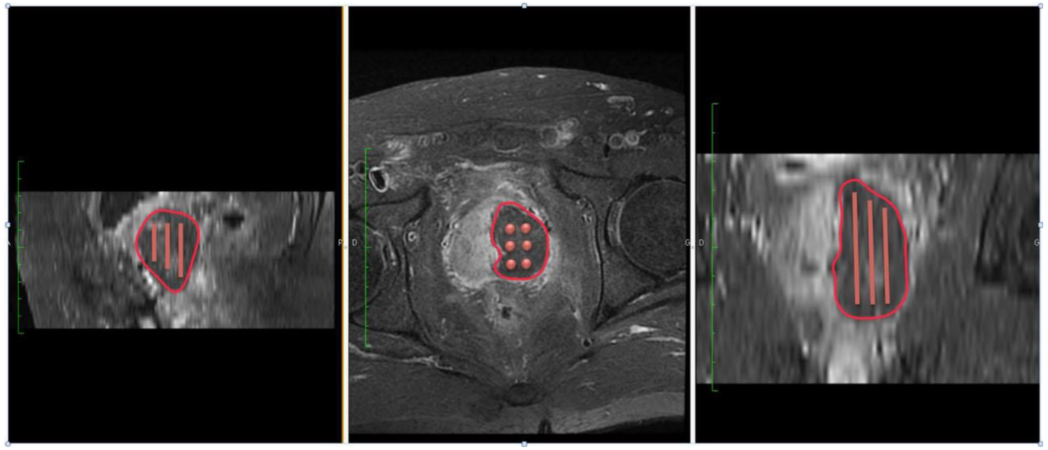

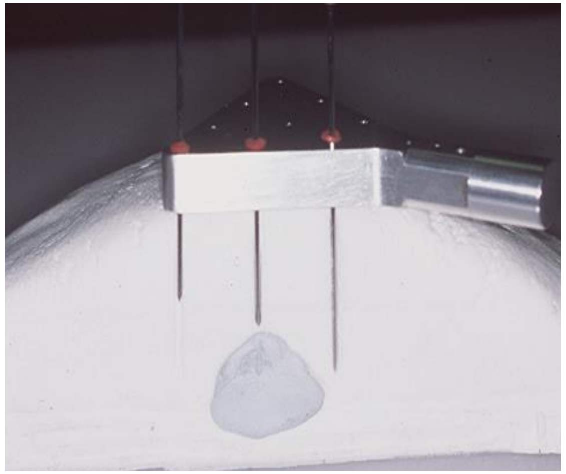

Images Courtesy of Colin Hopper. UCL UK

N. Betrouni et al. Vascular targeted photodynamic therapy with TOOKAD® Soluble (WST11) in localized prostate cancer: efficiency of automatic pre-treatment planningLasers Med Sci (2017) 32:1301–1307 DOI 10.1007/s10103-017-2241-7

## Speed

- CUDA-MCML (GPLv3) 2010 /Alerstam et al./
- MCX (GPLv3) 2009 /Fang, Boas/
- MCX-CL (GPLv3) 2012/2018 /Yu, Kaeli, Fang/
- FullMonteCUDA (BSD*) 2019 /Young-Schultz et al/
- MMCL (GPLv3) 2020 /Fang, Yan/

## Anatomical Accuracy

- MCML (BSD) 1993 /Wang,Jacques,Prahl/
- mcxyz (BSD) ?? /Jacques/
- tMCimg (BSD) 2002 /Boas et al./
- YMC3D (MIT) 2018 /Bjorgan et al./
- MOSE (non-free) 2004
- MMC/iMMC/DMMC (GPLv3) 2010 /Fang,Yan,/
- MCtet (unknown) 2018
- SVMC (part of MCX) 2021 /Yan, Fang/
- FullMonteSW (BSD*) 2018 /Cassidy et al./

## Usability

- VirtualPhotonics(BSD) 2010 /Cuccia et al./
- MCOnline (non-free) 2011
- MCmatlab (GPLv3) 2018 /Marti et al./
- ValoMC (MIT) 2019 /Leino et al./

Courtesy of Q. Fang, Boston

# Speed in performing light propagation models

Discrete method:

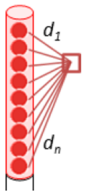


$$\phi(d) = \sum_{n=1}^{n_{sources}} \frac{P}{L_{diffuser\ length}} \cdot \frac{3.\mu_s'}{4.\pi.d_n} . e^{-d_n \cdot \mu_{eff}} . dl$$

Continuous method:

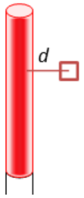


$$\phi(d) = P.\sqrt{\frac{2.\delta}{\pi.d}} . \frac{e^{-d/\delta}}{2\pi.\mu_a.\delta^2}$$

Table 2: Relative deviation computed for different source lengths; the mean is computed for all distances.

| | **Discrete method** | | **Continuous method** | |
|---|---|---|---|---|
| Source length (mm) | Mean (SD) | Max deviation | Mean (SD) | Max deviation |
| 10 | 4.94% (2.38%) | 8.00% | 11.16% (7.18%) | 19.10% |
| 15 | 4.70% (4.41%) | 15.38% | 24.31% (6.40%) | 32.77% |
| 20 | 1.05% (1.23%) | 4.24% | 27.40% (3.94%) | 30.56% |
| 30 | 1.70% (1.71%) | 5.56% | 28.61% (4.21%) | 32.65% |
| 40 | 0.91% (1.46%) | 5.00% | 30.12% (5.14%) | 37.50% |
| 50 | 1.89% (1.34%) | 4.49% | 29.48% (4.77%) | 35.96% |


C. Dupont et al. 5-ALA Photodynamic Therapy in Neurosurgery, Towards the Design of a Treatment Planning System: A Proof of Concept. Innovation and Research in BioMedical engineering, Elsevier Masson, 2016, 10.1016/j.irbm.2016.11.002. hal-01403867

# What Dose is Monitored or Planed for ?

- Power or photon density, photosensitizer bleaching.

- Outcome determining parameter, direct or indirect reporter.

Direct dose

Triplet dose

Implicit dose

Explicit dose

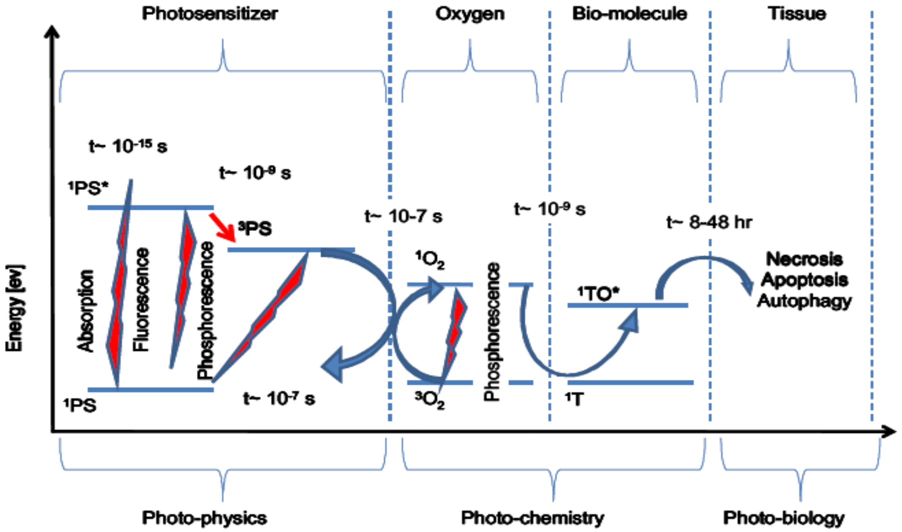


**Biological response**

B. C. Wilson, et al. Lasers Med. Sci. 12(3), 182–199 (1997).

# Imaging based PDT Efficacy monitoring

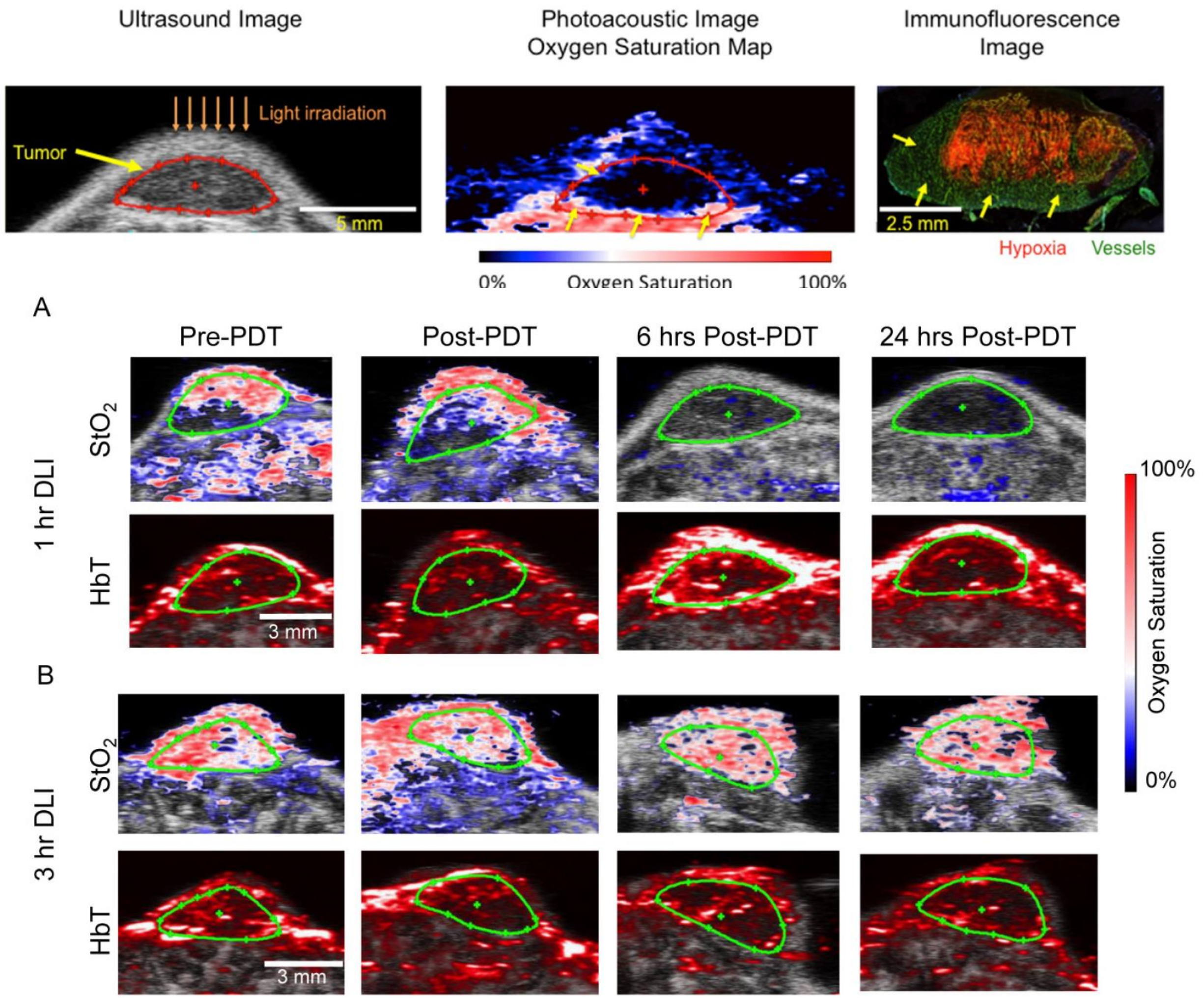


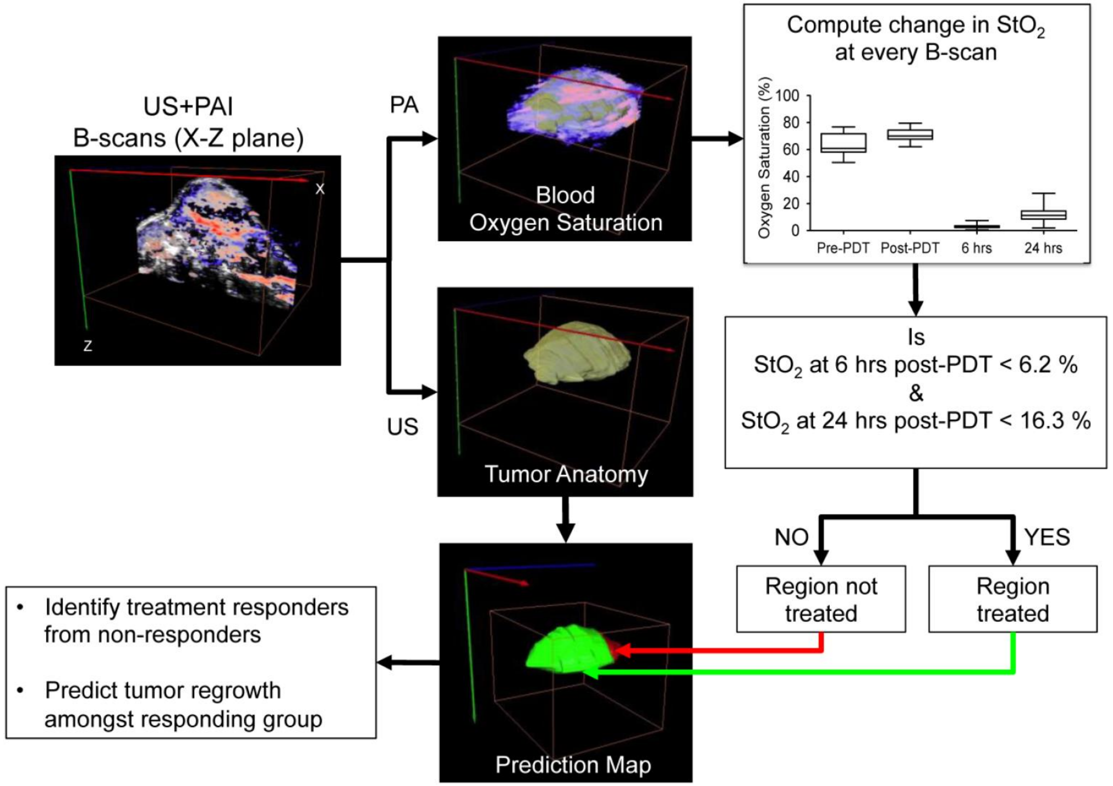


Mallidi S et al. Prediction of Tumor Recurrence and Therapy Monitoring Using Ultrasound-Guided Photoacoustic Imaging Theranostics 2015; 5(3): 289-301. doi: 10.7150/thno.10155

# Apoptosis Imaging based PDT Monitoring

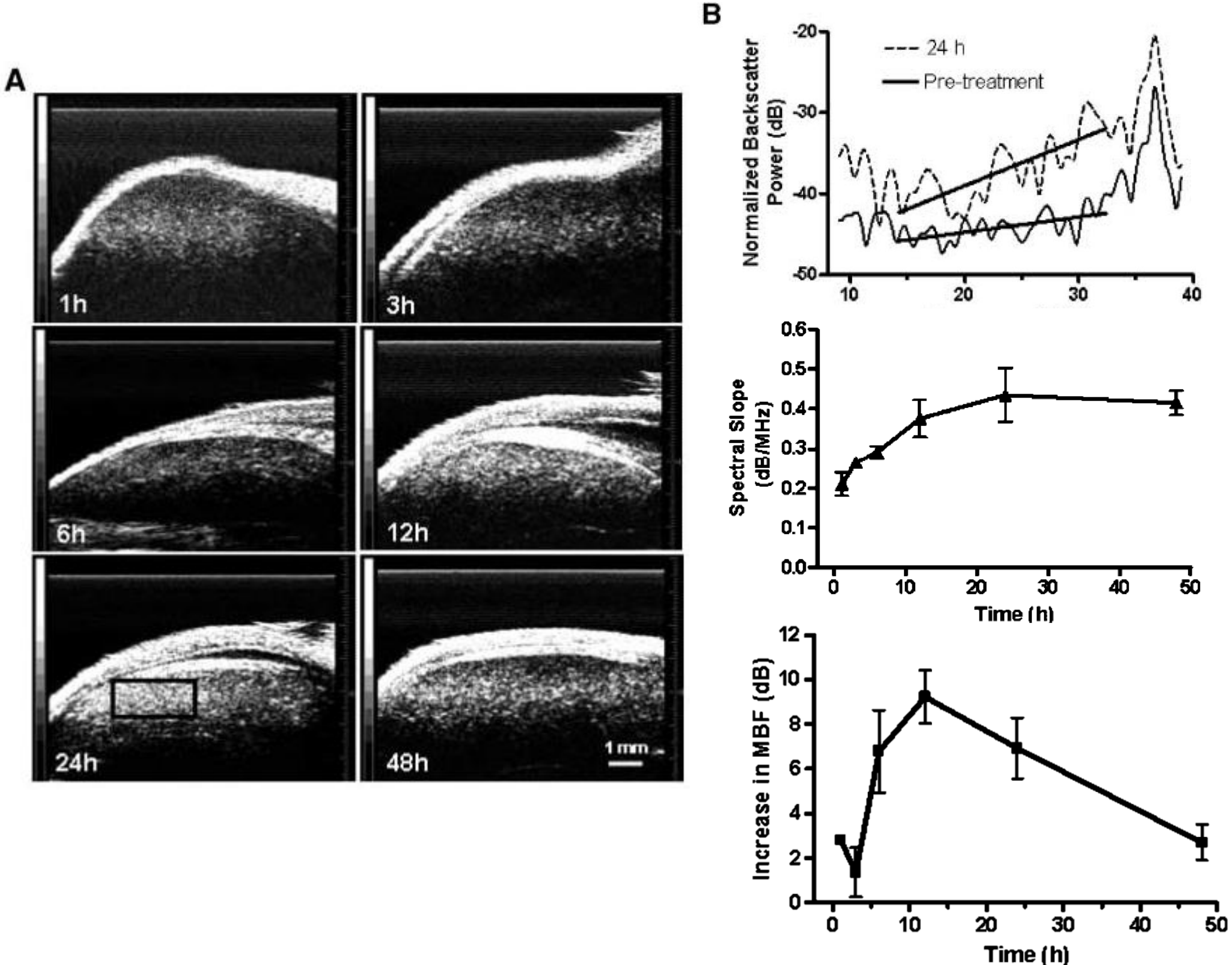


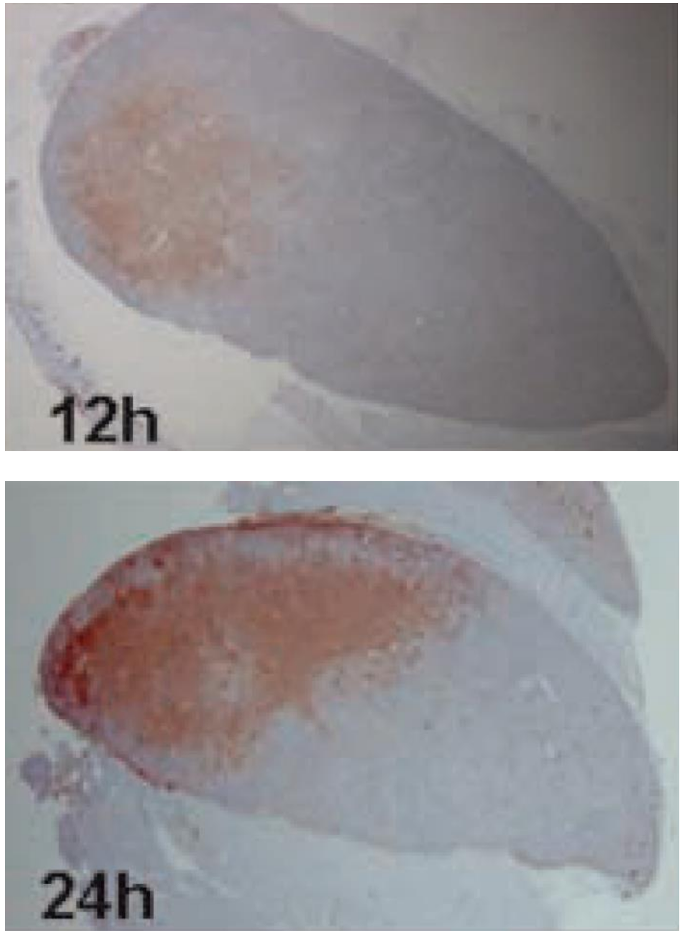


Banihashemi B et al. Ultrasound Imaging of Apoptosis in Tumor Response: Novel Preclinical Monitoring of Photodynamic Therapy Effects. Cancer Res 2008;68(20):8590–6

# Monitoring Hemodynamic changes online

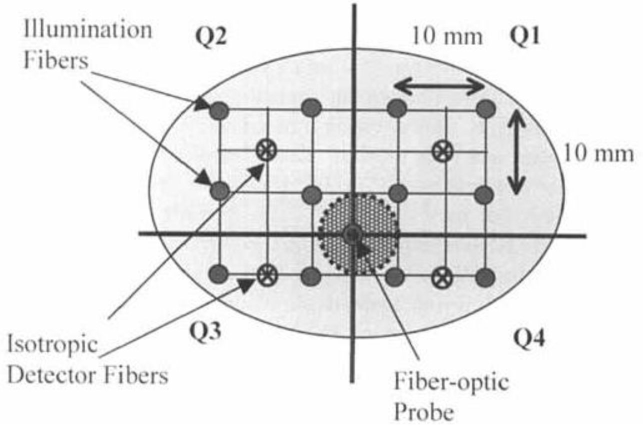


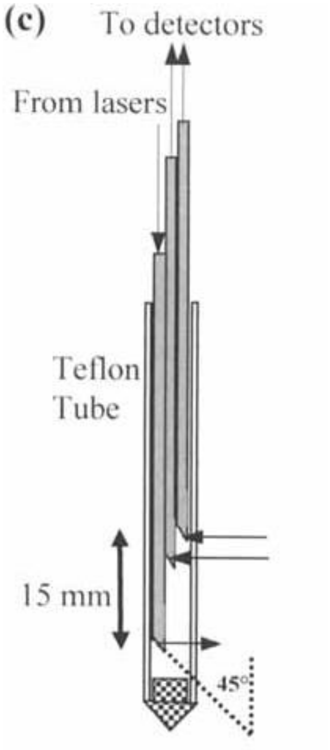


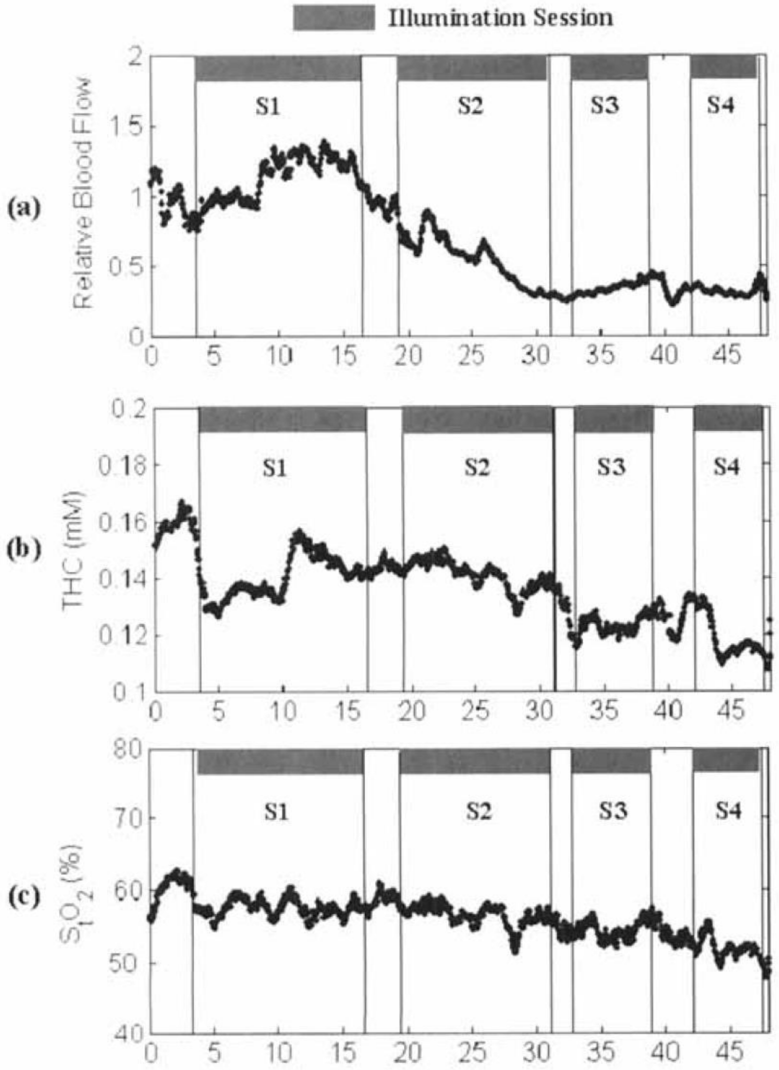


Guoqiang Y, et al. Real-time *In Situ* Monitoring of Human Prostate Photodynamic Therapy with Diffuse Light Photochemistry and Photobiology, 2006, 82: 1279-1 284

# Photosensitizer and Sensor Combination

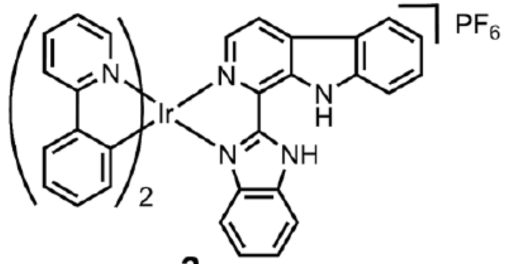


**2**

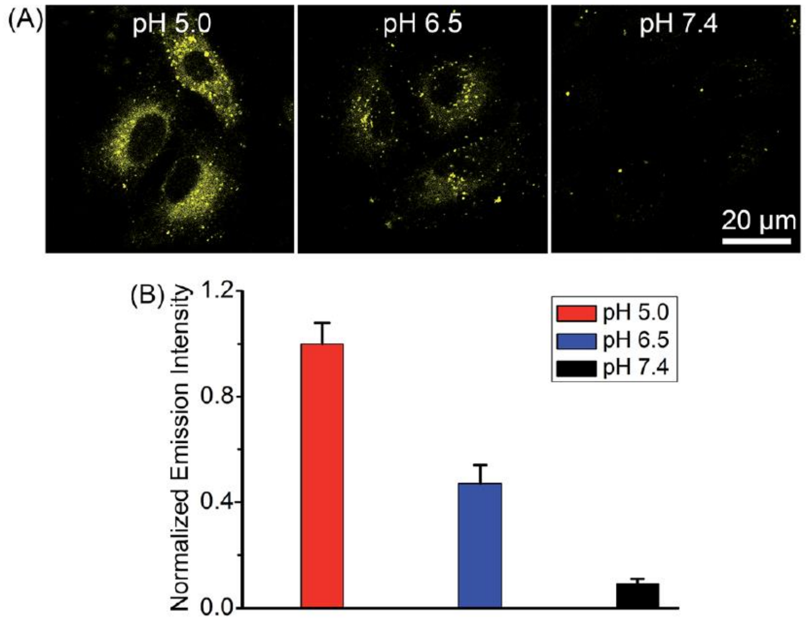


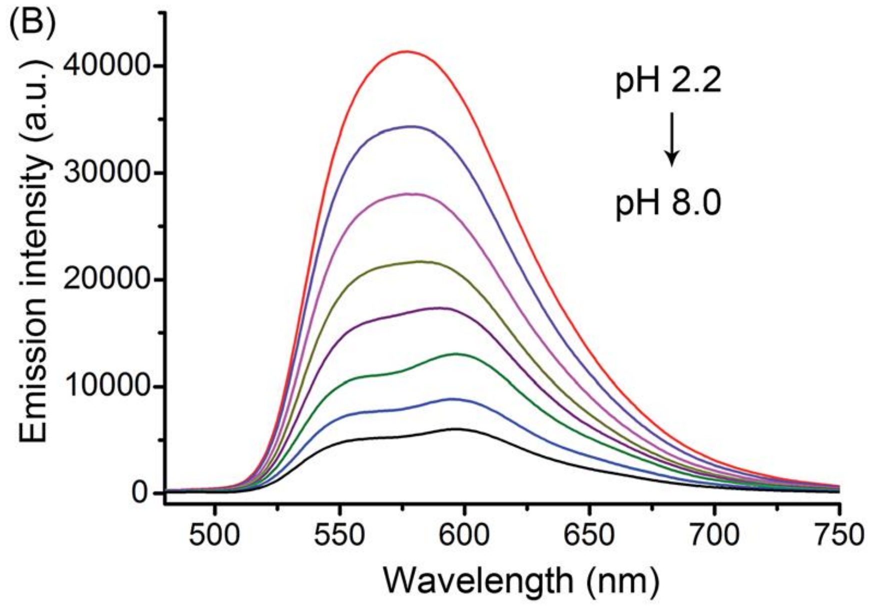


Liang H et al. Cyclometalated iridium(III) complexes as lysosometargeted photodynamic anticancer and real-time tracking agents Chem. Sci., 2015, 6, 5409 10.1039/c5sc01955a

# What Dose is Monitored or guides Planning ?

Direct dose

Triplet dose

Implicit dose

Explicit dose

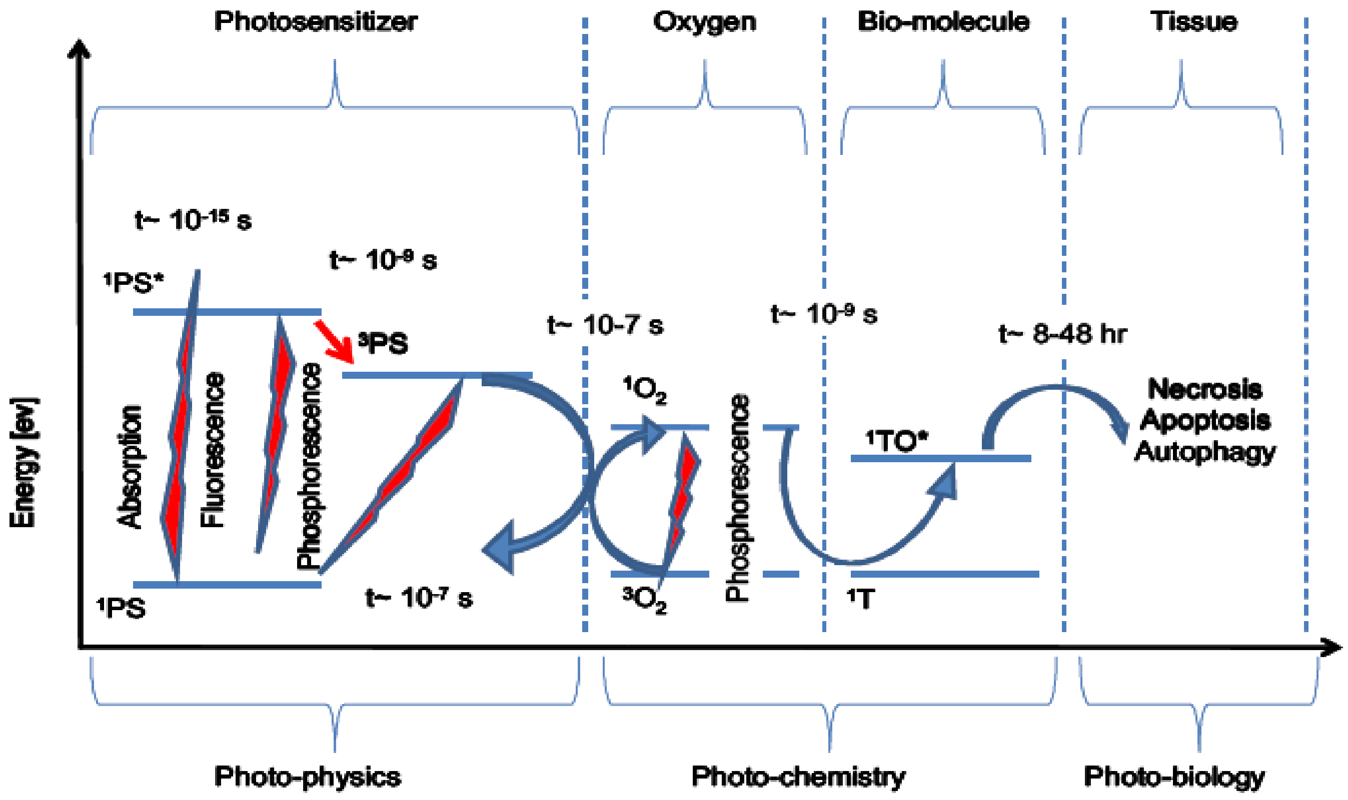


Wilson BC et al. Lasers Med. Sci. 12(3), 182–199 (1997).

# Indirect Singlet Oxygen Dose Metric

$$[^1O_2](t) = N\sigma[S_0]\Phi_D \frac{\tau_D}{\tau_T - \tau_D}[\exp(-t/\tau_T) - \exp(-t/\tau_D)]$$

$$[^1O_2] = S_\Delta \phi_t I_{a(i)} \left(\frac{[^3O_2]}{k_p/k_{ot} + [^3O_2]}\right)\left(\frac{1}{k_d + k_{oa}[A]}\right)$$

$$\int L_{1270}(t)\, dt = \frac{N\sigma[S_0]\Phi_D\tau_D}{\tau_R}$$

$$\text{Dose} = \frac{1}{\tau_\Delta k_{os}\delta}([S_0]_0 - [S_0](T)) \quad \text{for } [S_0] \ll \delta$$

$$\text{Dose} = \frac{1}{\tau_\Delta k_{os}} \ln\left(\frac{[S_0]_0}{[S_0](T)}\right) \quad \text{for } [S_0] \gg \delta.$$

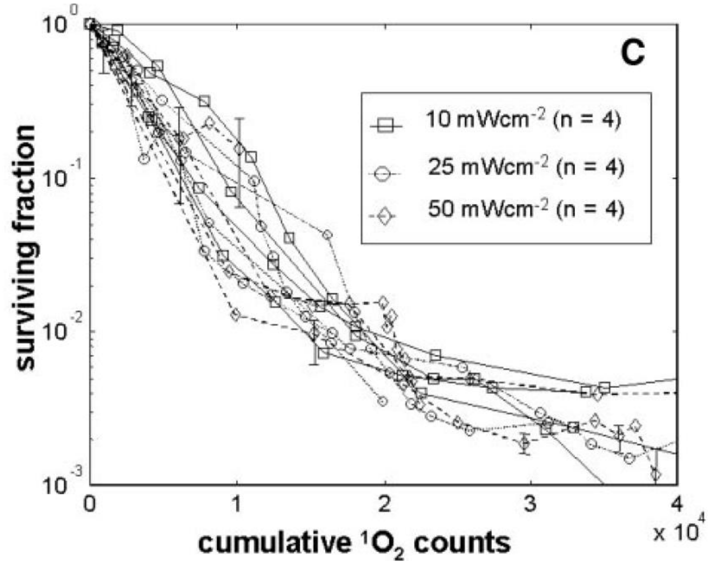


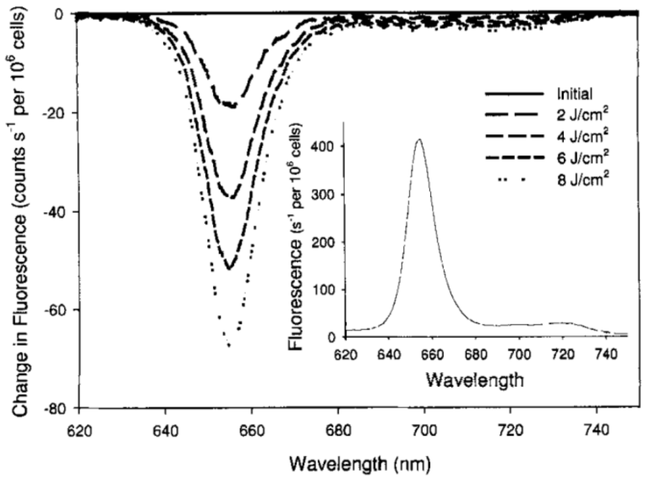


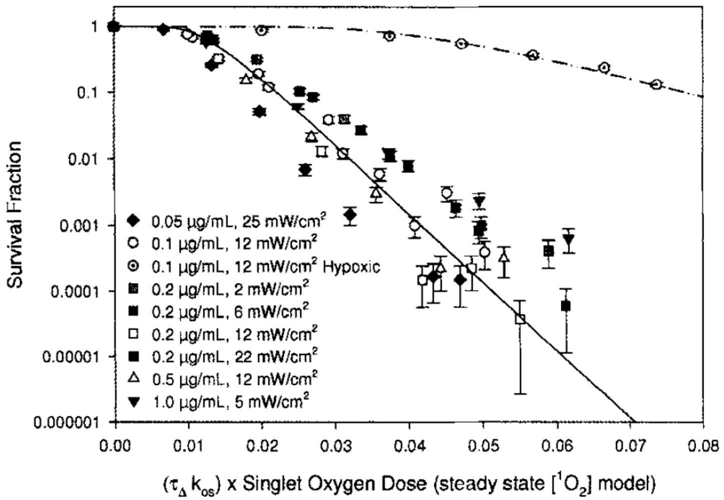


In Vitro Tests of the Validity of Singlet Oxygen Luminescence Measurements as a Dose Metric in Photodynamic Therapy CANCER RESEARCH 63, 7986–7994, November 15, 2003

Dysart JS et al. Calculation of Singlet Oxygen Dose from Photosensitizer Fluorescence and Photobleaching During mTHPC Photodynamic Therapy of MLL Cells? Photochemistry and Photobiology, 2005, 81 : 196-205

# Multiparameter Dose approach

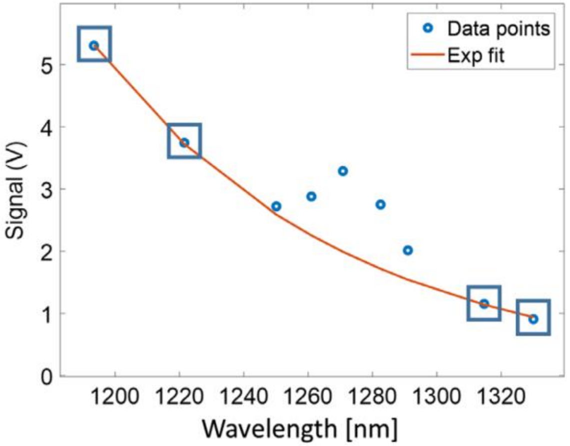


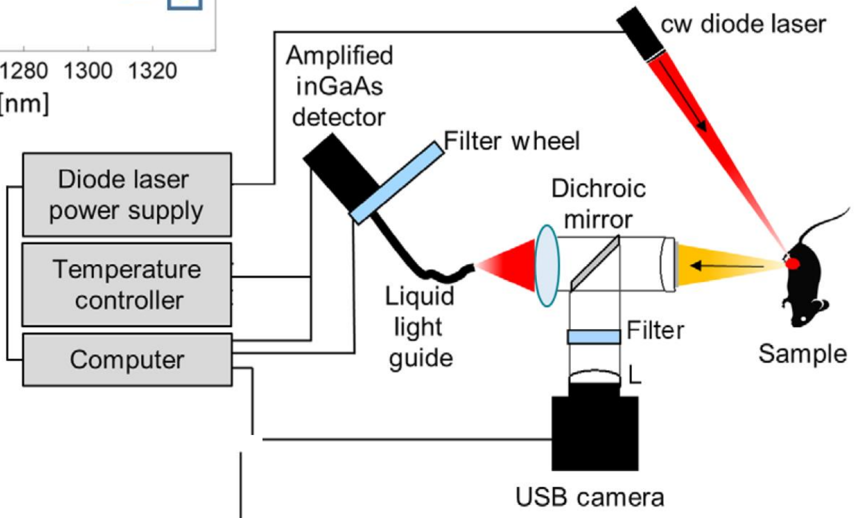


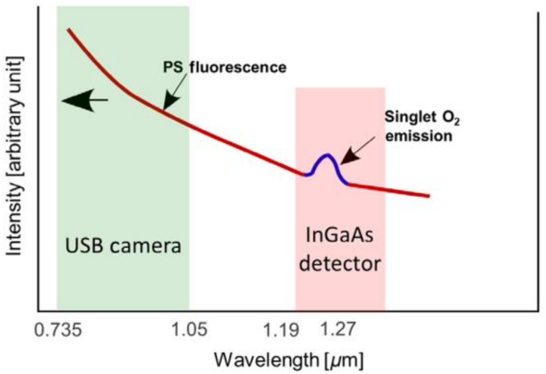


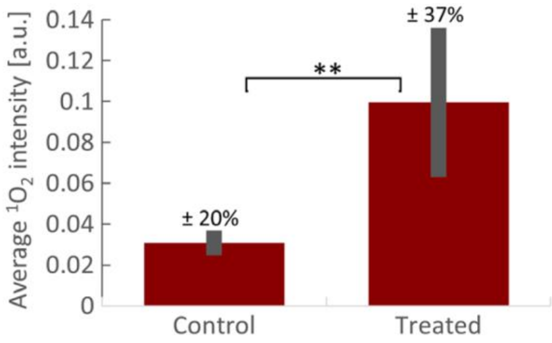


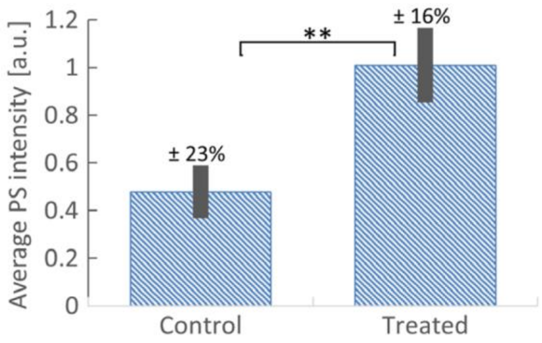


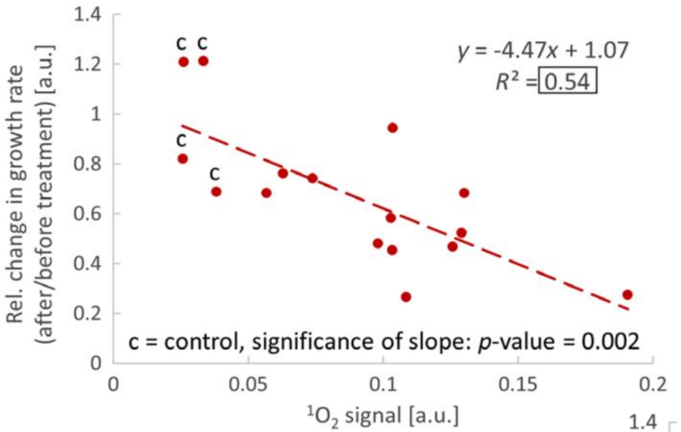


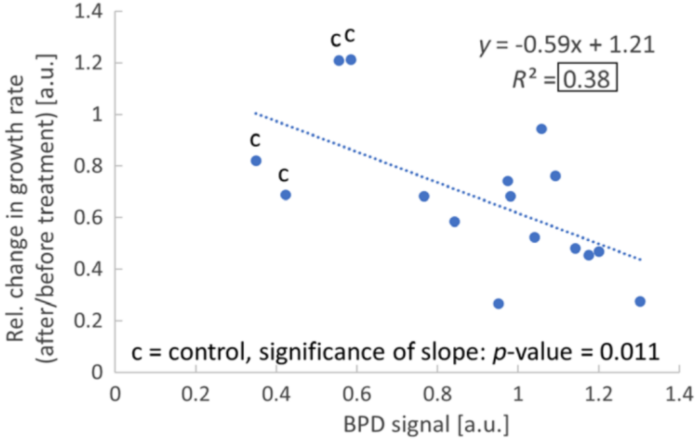


Moritz JT et al. Multispectral singlet oxygen and photosensitizer luminescence dosimeter for continuous photodynamic therapy dose assessment during treatment J. Biomed. Opt. 25(6), 063810 (2020), doi: 10.1117/1.JBO.25.6.063810

# Intra-operative fluence rate measurements

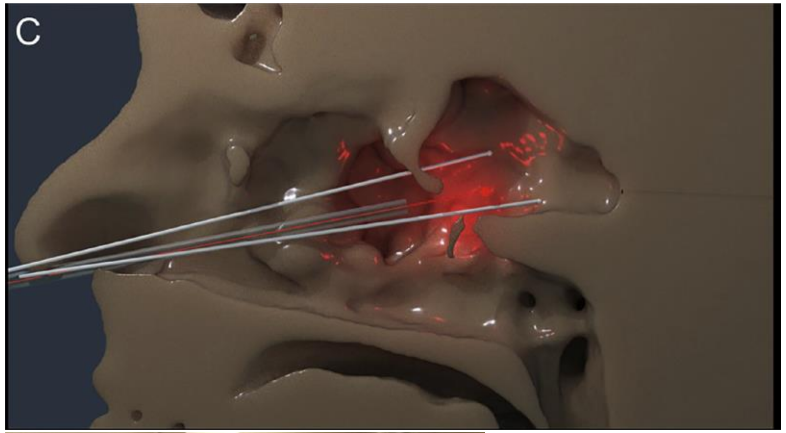



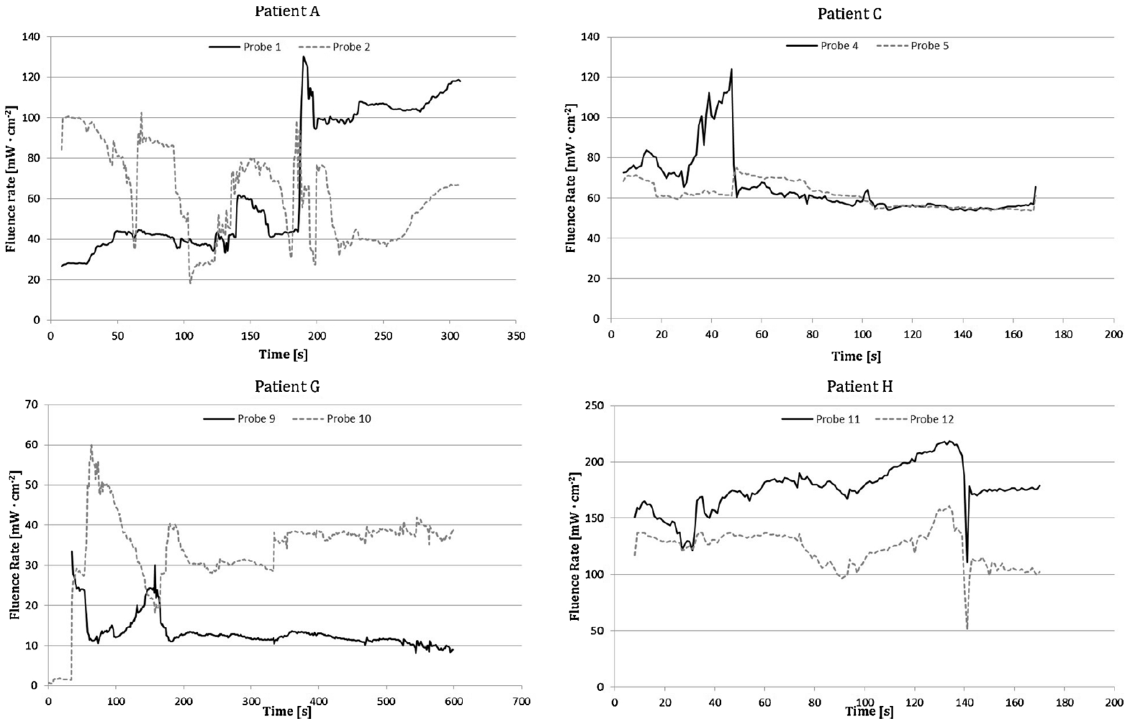


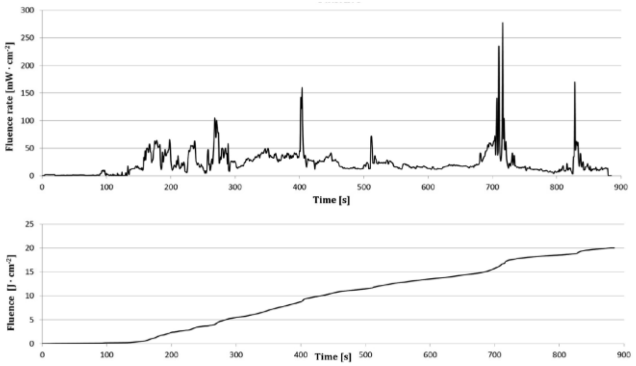


van Doeveren TEM et al. Intra-cavity Photodynamic Therapy for malignant tumors of the paranasal sinuses: An *in vivo* light dosimetry study Photodiagnosis and Photodynamic Therapy 32 (2020) 101972

# Intermezzo

- Treatment progress monitoring appears feasible
  - Φ (r, t), [PS] (r, Φ) , [$^3O_2$] (r, Φ) , [$^1O_2$] (Φ)
  - What is the target PDT dose?

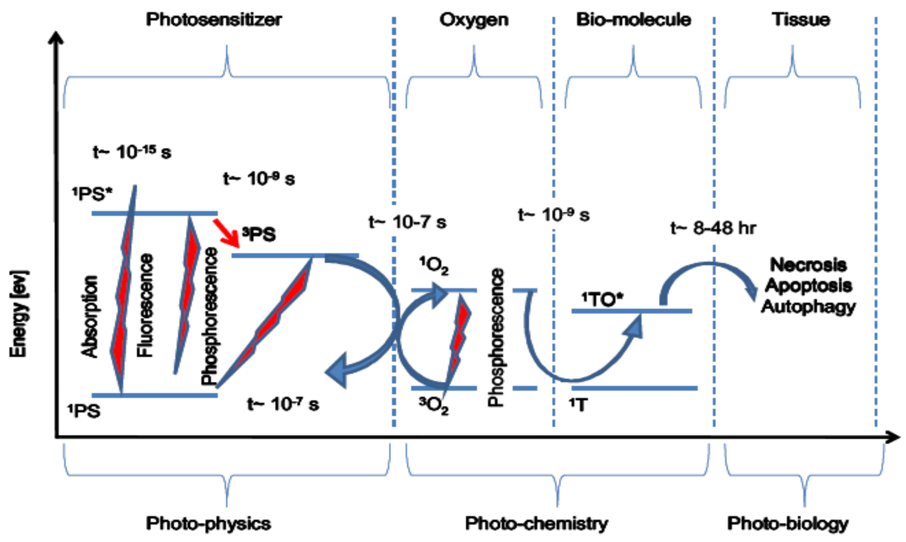


- Was the original plan for PDT
  - Optimal light delivery (outcome)
  - Personalized
  - What is the target PDT dose?

# Photochemical Dosimetry

| Simulation Parameters for Photofrin® | |
|---|---|
| $k_0 = (1.895 \times 10^{-2})$*(fluence rate) $s^{-1}$ | $\delta(\mu M) = 0$ |
| $k_1 = 1.2 \times 10^5\ \mu M^{-1}\ s^{-1}$ | $S_\Delta = 1$ |
| $k_2 = 100\ \mu M^{-1}\ s^{-1}$ | $[S_0\ (t{=}0)] = 8.5\ \mu M$ |
| $k_3 = 2 \times 10^7\ s^{-1}$ | $[^3O_2\ (t{=}0)] = 83\ \mu M$ |
| $k_4 = 1250\ s^{-1}$ | $[A\ (t{=}0)] = 830\ \mu M$ |
| $k_5 = 8 \times 10^7\ s^{-1}$ | $g = 1.0\ \mu M/s$ |
| $k_6 = 1 \times 10^6\ s^{-1}$ | $\sigma(S_0\text{-}S_1) = 5.978 \times 10^{-18}\ cm^2$ |
| $k_7 = 2.6 \times 10^6\ \mu M^{-1}\ s^{-1}$ | |

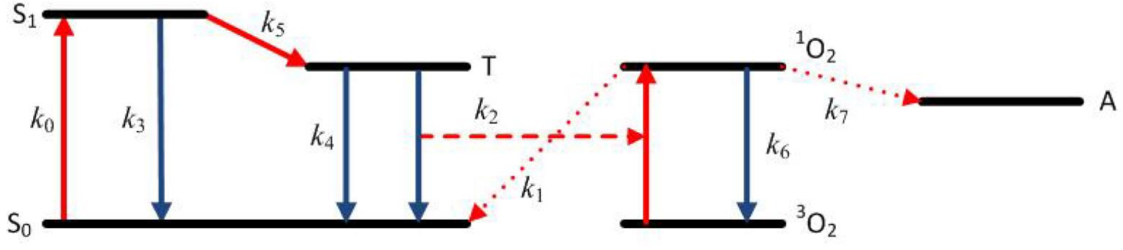


$$\frac{d[S_0]}{dt} = -k_0[S_0] - k_1[^1O_2]([S_0]+\delta) + k_2[T][^3O_2] + k_3[S_1] + k_4[T]$$

$$\frac{d[S_1]}{dt} = -(k_3+k_5)[S_1] + k_0[S_0]$$

$$\frac{d[T]}{dt} = -k_2[T][^3O_2] - k_4[T] + k_5[S_1]$$

$$\frac{d[^3O_2]}{dt} = -S_\Delta k_2[T][^3O_2] + k_6[^1O_2] + g\left(1 - \frac{[^3O_2]}{[^3O_2](t=0)}\right)$$

$$\frac{d[^1O_2]}{dt} = -k_1([S_0]+\delta)[^1O_2] + S_\Delta k_2[T][^3O_2] - k_6[^1O_2] - k_7[A][^1O_2]$$

$$\frac{d[A]}{dt} = -k_7[A][^1O_2]$$

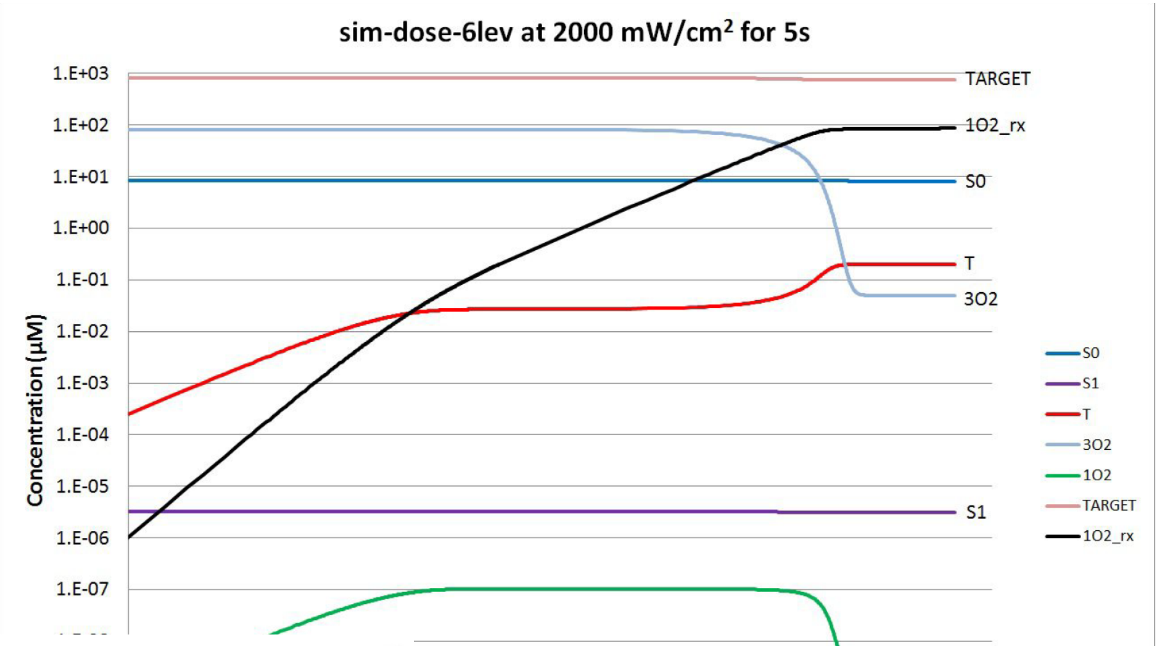


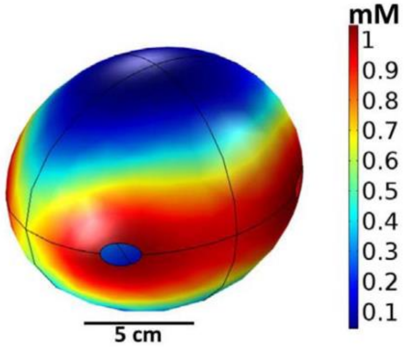


Beeson K et al. Overview of computational simulations for PDT treatments based on optimal choice of singlet oxygen Optical Methods for Tumor Treatment and Detection: Mechanisms and Techniques in Photodynamic Therapy XXVI, 100470R 2017 doi: 10.1117/12.2252552

# Dosie™device

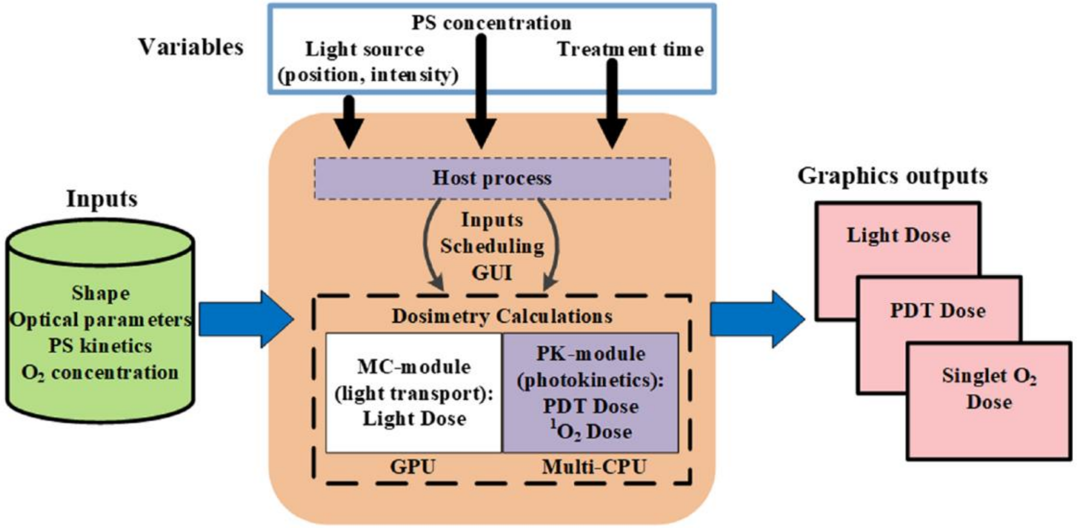


**Fig. 1** Schematic diagram for Dosie™ integrated computer and software computational device. The computer includes both a GPU and a multicore CPU. The software first performs a MC simulation of light transport that is followed by a PK simulation.

$$\frac{d[S_0]}{dt} + \left(\xi\sigma\frac{\phi([S_0]+\delta)[^3O_2]}{[^3O_2]+\beta}\right)[S_0] = 0$$

$$\frac{d[^1O_2]_{rx}}{dt} - \left(\xi\frac{\phi[S_0][^3O_2]}{[^3O_2]+\beta}\right) = 0$$

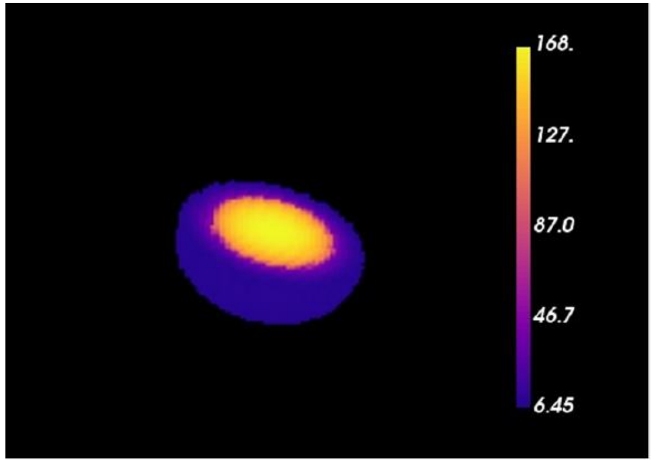


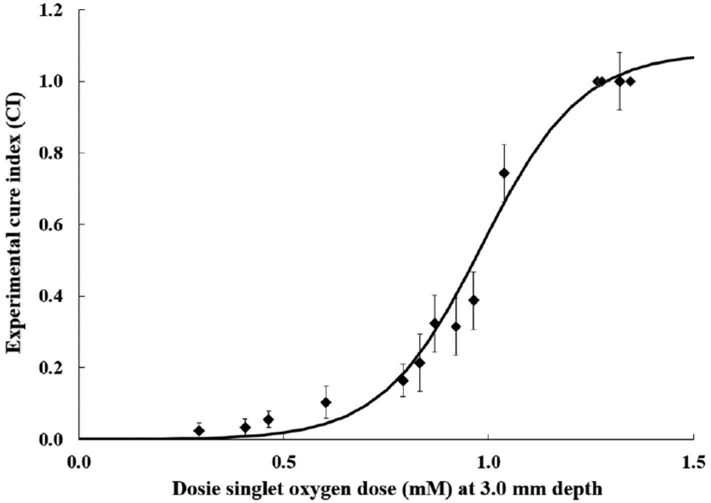


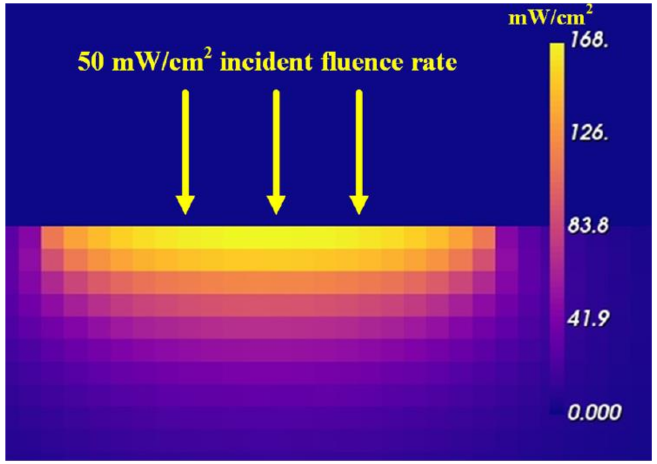


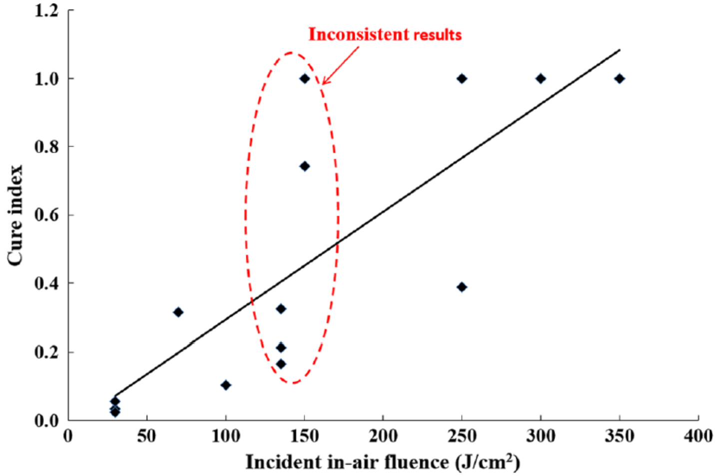


Beeson KW et al. Validation of combined Monte Carlo and photokinetic simulations for the outcome correlation analysis of benzoporphyrin derivative-mediated photodynamic therapy on mice. J. Biomed. Opt. 24(3), 035006 (2019), doi: 10.1117/1.JBO.24.3.035006.

# What do we know about the inputs for iPDT optimization/personalization

- Shape
  - Medical imaging helps
- Optical Properties
  - Spatially resolved online monitoring
- PS Kinetics
  - fMRI BOLD
- Oxygen Concentration
  - DRS, fMRI BOLD
- Biological response of different tissues
  - Very little.

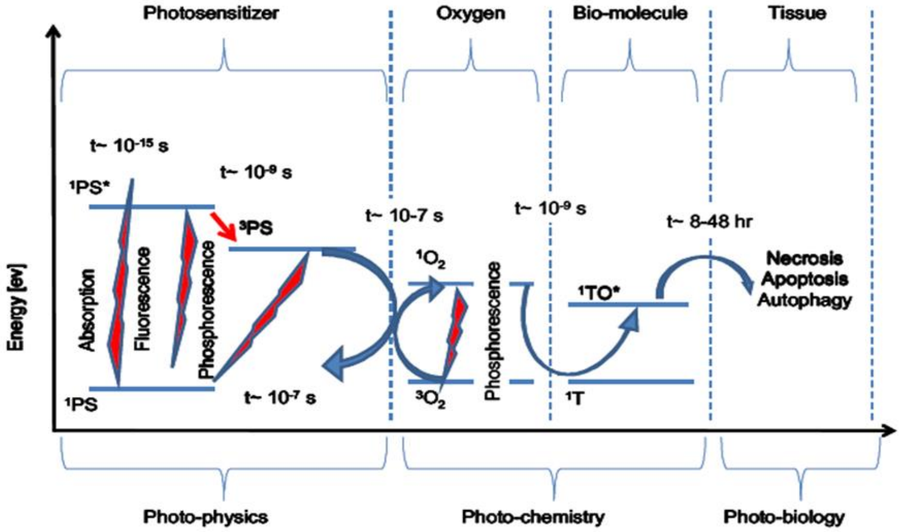

# Free Space Light source placement

## Offline planning

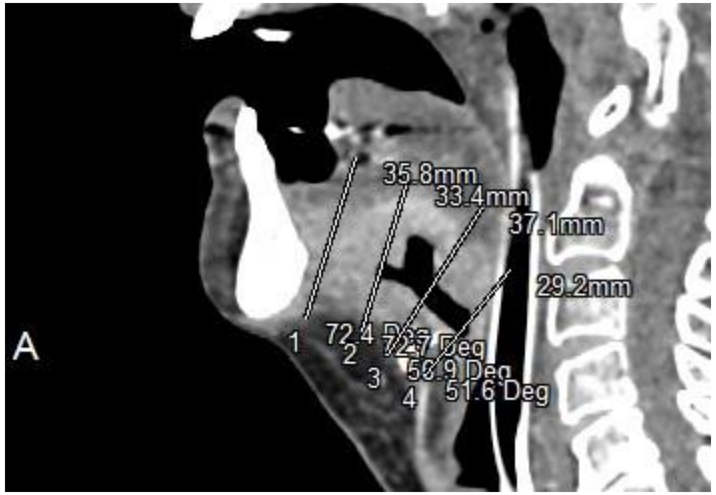


Planned sagittal section

Rigid registration and non deformation allows for robotic needle insertion

Images Courtesy of Colin Hopper. UCL UK

## Online Monitoring CT

First in-plane needle insertion

Final sagittal section appearance

## Online Monitoring CT

## Online Monitoring US

Jerjes et al. 2009 Lasers in Medical Science

# Free Space Light source placement

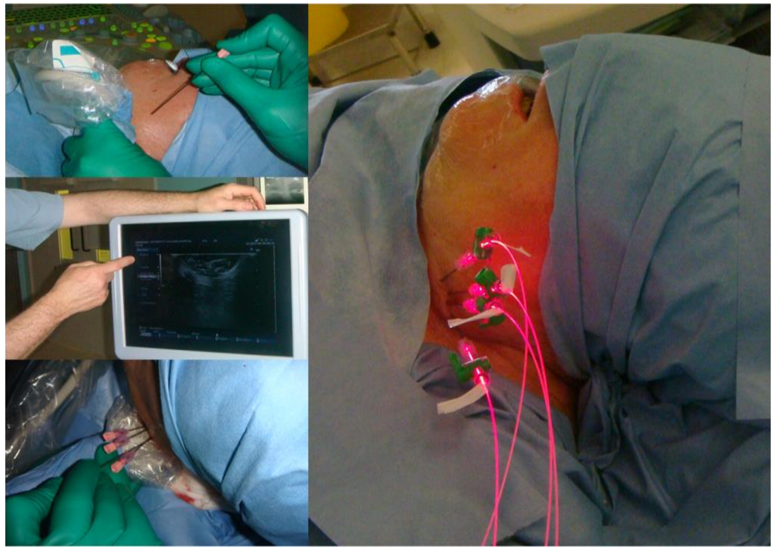

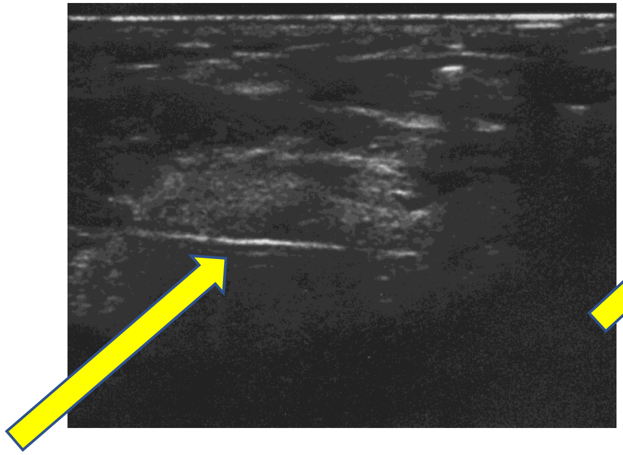

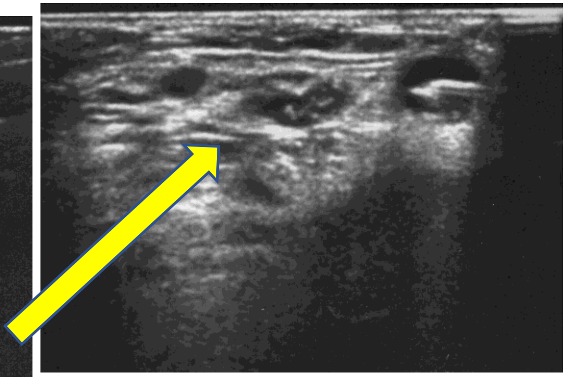

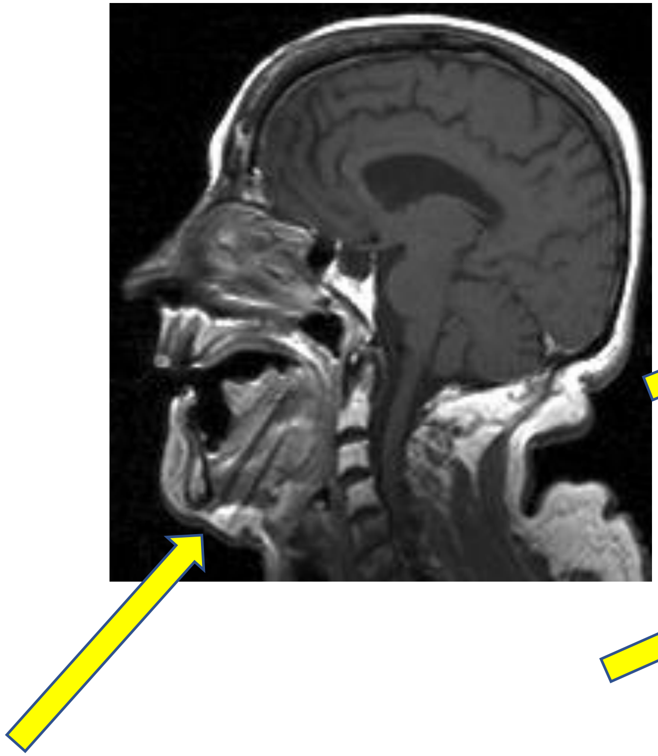

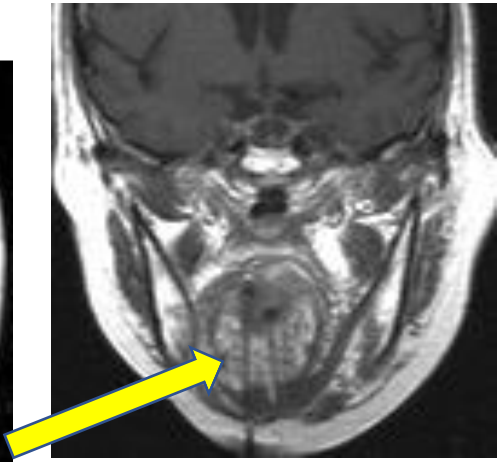

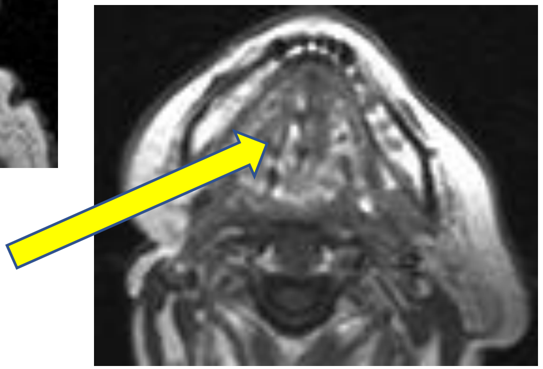

Images Courtesy of Colin Hopper. UCL UK

# Robotic controlled light source placement

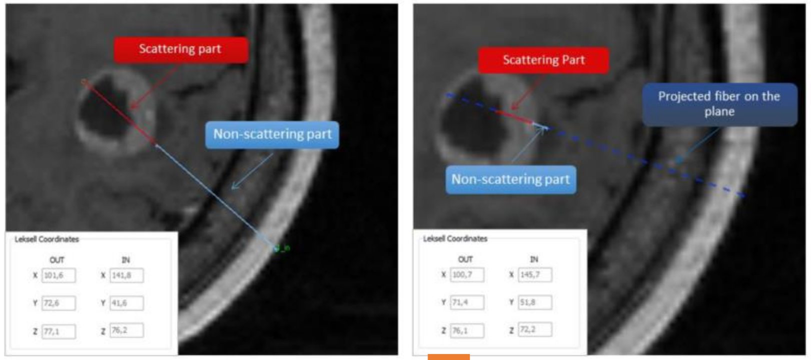


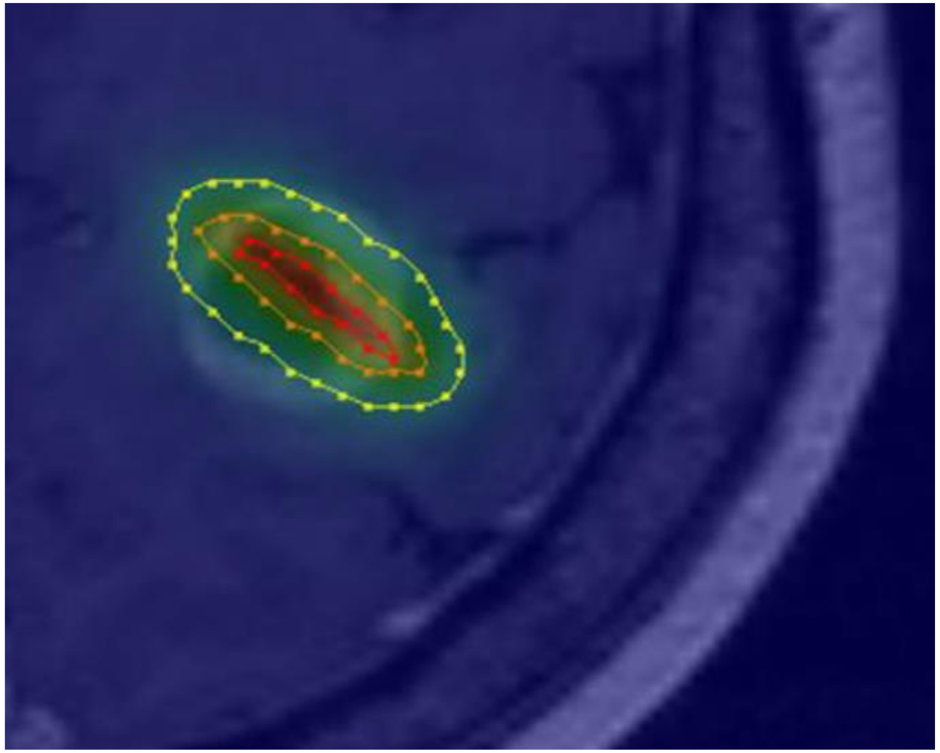

DICOM loading → Leksell registration → Target volume definition → Light sources properties definition; Insertion planning → Dosimetry computing → Fluence value definition; Treatment time estimation

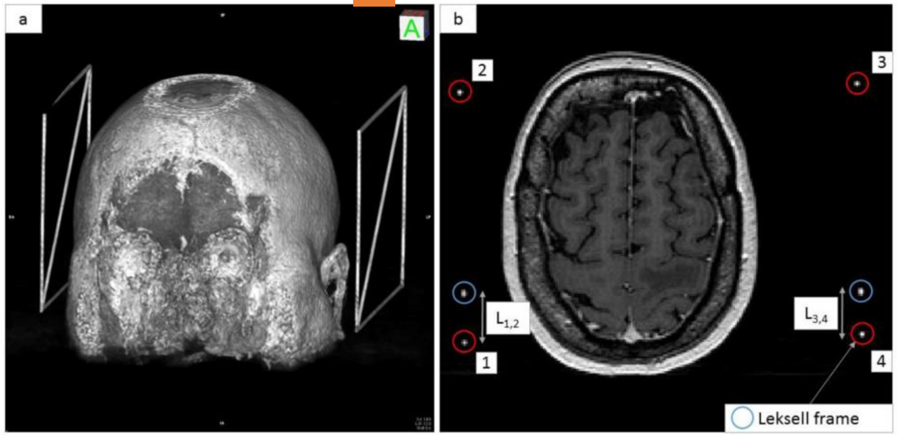


$$\phi(d) = P.\sqrt{\frac{2.\delta}{\pi.d}}.\frac{e^{-d/\delta}}{2\pi.\mu_a.\delta^2}$$

C. Dupont et al. .5-ALA Photodynamic Therapy in Neurosurgery ,Towards the Design of a Treatment Planning System :A Proof of Concept. Innovation and Research in BioMedical engineering, 2016,10.1016/j.irbm.2016.11.002.hal-01403867

# Planning in the absence true $\mu_a$, $\mu_s$ and g

**Table 1.** Parameters specifying thereduced scattering coefficient of tissues: $a = \mu'_{s500\ \mathrm{nm}}$, such that $\mu'_s(\lambda) = a(\lambda/500\ \mathrm{nm})^{-b}$, equation (1); $aa = \mu'_{s500\ \mathrm{nm}}$, such that $\mu'_s(\lambda) = aa(f_{\mathrm{Ray}}(\lambda/500\ \mathrm{nm})^{-b} + f_{\mathrm{Mie}}(\lambda/500\ \mathrm{nm})^{-b_{\mathrm{Mie}}})$, equation (2); and $f_{\mathrm{Mie}} = 1 - f_{\mathrm{Ray}}$. (na = not available.)

| # | $a$ (cm$^{-1}$) | $b$ | $a'$ (cm$^{-1}$) | $f_{\mathrm{Ray}}$ | $b_{\mathrm{Mie}}$ | Ref. | Tissue |
|---|---|---|---|---|---|---|---|
| Skin | | | | | | | |
| 1 | 48.9 | 1.548 | 45.6 | 0.22 | 1.184 | Skin | Anderson *et al* 1982 |
| 2 | 47.8 | 2.453 | 42.9 | 0.76 | 0.351 | Skin | Jacques 1996 |
| 3 | 37.2 | 1.390 | 42.6 | 0.40 | 0.919 | Skin | Simpson *et al* 1998 |
| 4 | 60.1 | 1.722 | 58.3 | 0.31 | 0.991 | Skin | Saidi *et al* 1995 |
| 5 | 29.7 | 0.705 | 36.4 | 0.48 | 0.220 | Skin | Bashkatov *et al* 2011 |
| 6 | 45.3 | 1.292 | 43.6 | 0.41 | 0.562 | Dermis | Salomatina *et al* 2006 |
| 7 | 68.7 | 1.161 | 66.7 | 0.29 | 0.689 | Epidermis | Salomatina *et al* 2006 |
| 8 | 30.6 | 1.100 | na | na | na | Skin | Alexandrakis *et al* 2005 |
| Brain | | | | | | | |
| 9 | 40.8 | 3.089 | 40.8 | 0.00 | 3.088 | Brain | Sandell and Zhu 2011 |
| 10 | 10.9 | 0.334 | 13.3 | 0.36 | 0.000 | Cortex (frontal lobe) | Bevilacqua *et al* 2000 |
| 11 | 11.6 | 0.601 | 15.7 | 0.53 | 0.000 | Cortex (temporal lobe) | Bevilacqua *et al* 2000 |
| 12 | 20.0 | 1.629 | 29.1 | 0.81 | 0.000 | Astrocytoma of optic nerve | Bevilacqua *et al* 2000 |

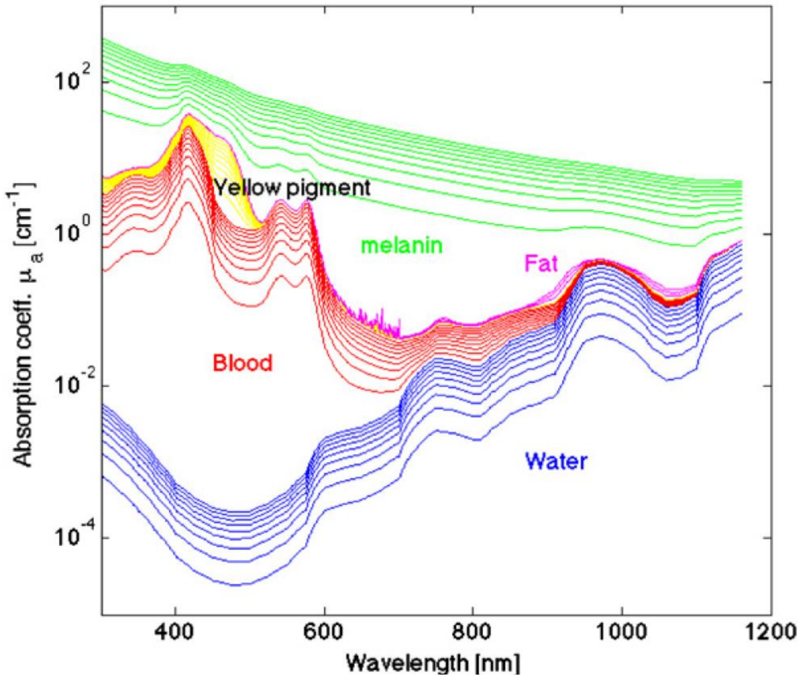


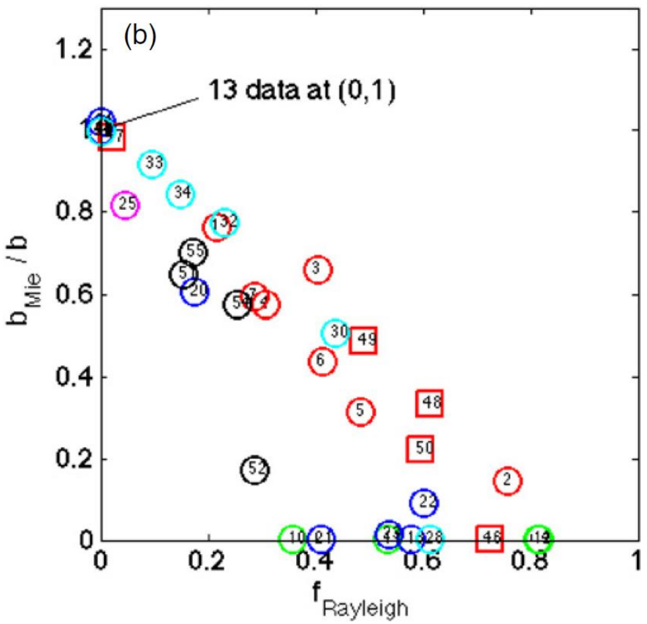


$$\mu_a = BS\mu_{a.\mathrm{oxy}} + B(1-S)\mu_{a.\mathrm{deoxy}} + W\mu_{a.\mathrm{water}} + F\mu_{a.\mathrm{fat}} + M\mu_{a.\mathrm{melanosome}} + 2.3C_{\mathrm{bili}}\varepsilon_{\mathrm{bili}} + 2.3C_{\beta\mathrm{C}}\varepsilon_{\beta\mathrm{C}}.$$

| | |
|---|---|
| $S$ | HGb oxygen saturation of mixed arterio-venous vasculature |
| $B$ | average blood volume fraction ($f_{v.\mathrm{blood}}$) |
| $W$ | water content ($f_{v.\mathrm{water}}$) |
| Bili | bilirubin concentration ($C$ (M)) |
| $\beta$C | $\beta$-carotene concentration ($C$ (M)) |
| $F$ | fat content ($f_{v.\mathrm{fat}}$) |
| $M$ | melanosome volume fraction ($f_{v.\mathrm{melanosome}}$), or alternatively the molar concentration of melanin monomers ($C$ (M)). |

Jacques SL Optical properties of biological tissues: a review Phys. Med. Biol. 58 (2013) R37–R61

# Optical Parameter Quantification

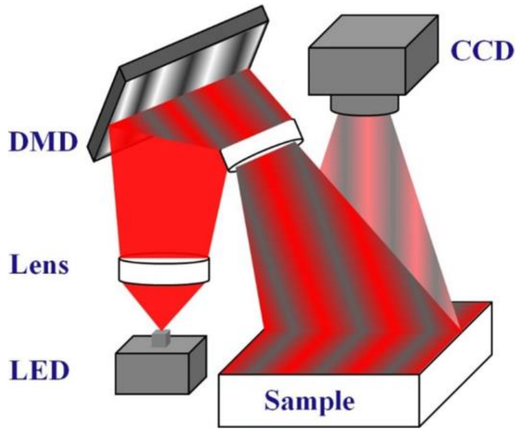


$$MTF(f_x) = \frac{M_R(f_x)}{M_S(f_x)}$$

$$M_S(f_x) = A_S^{(f_x)}/A_S^{(0)} \text{ and } M_R(f_x) = A_R^{(f_x)}/A_R^{(0)}$$

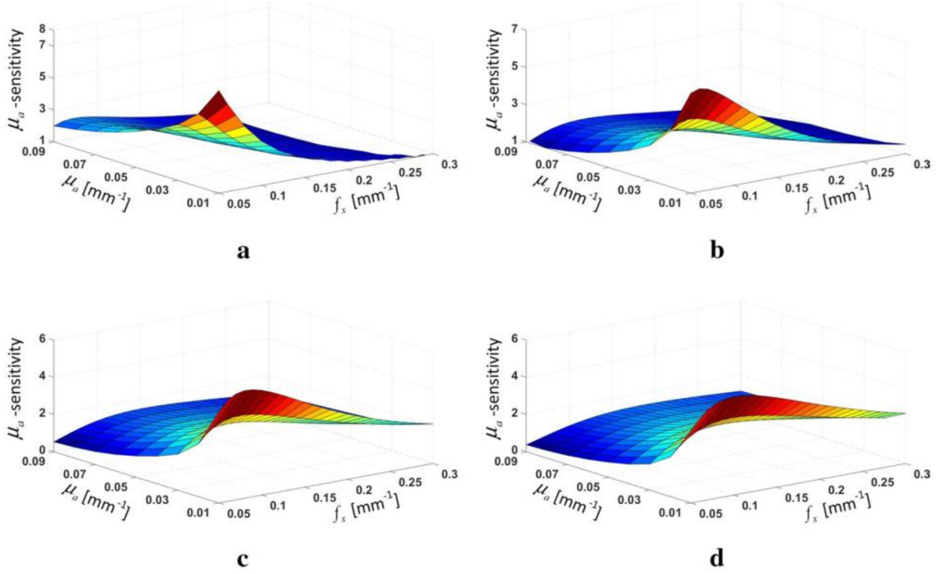


$$\phi_n(\mu_a,\mu_s,r)=\frac{1}{4\pi}\sum_{i=1}^{\frac{N+1}{2}}\upsilon_i(\mu_a,\mu_s)G_i(\omega_i(\mu_a,\mu_s))I_n(\upsilon_i(\mu_a,\mu_s))\kappa_n(\upsilon_i(\mu_a,\mu_s)r)$$

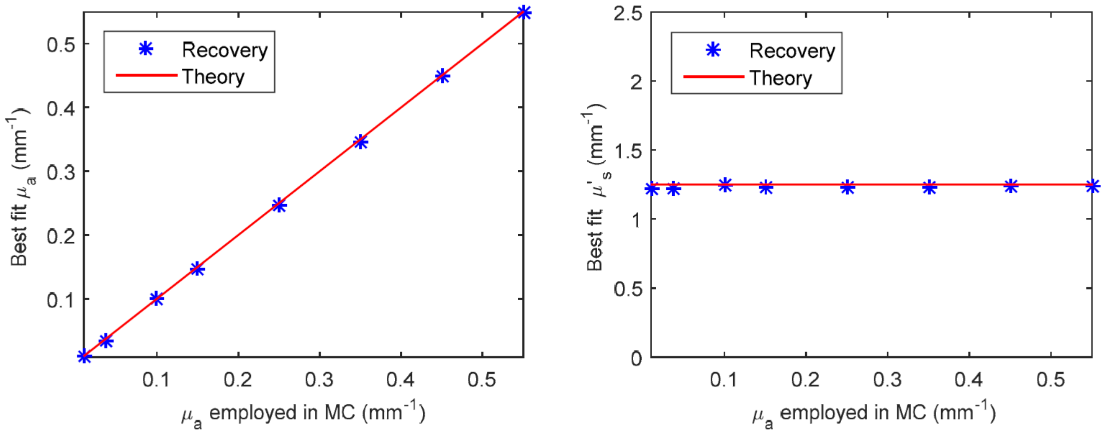


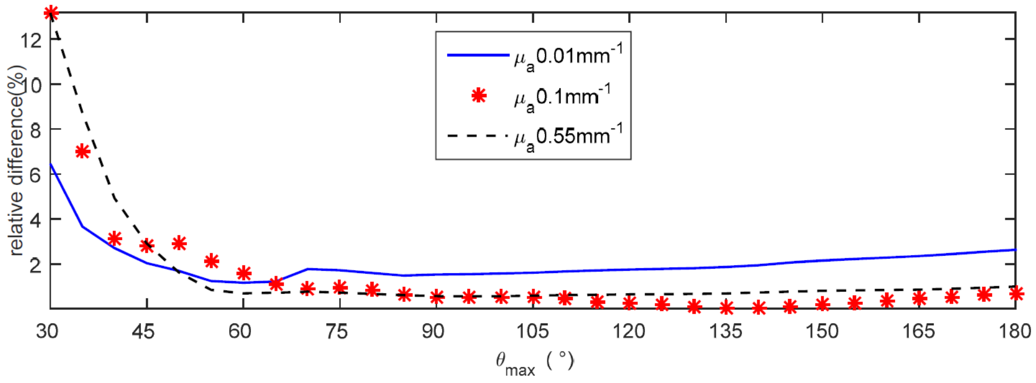


Chen W et al. Reference-free determination of tissue absorption coefficient by modulation transfer function characterization in spatial frequency domain *BioMed Eng OnLine (2017) 16:100*

Liu L et al. Interstitial optical parameter quantification of turbid medium based on CW radiance measurements. SPIE 10024, Optics in Health Care and Biomedical Optics VII, 1002436 2016; doi: 10.1117/12.2246053

# Experimental Methods for Light Dose Profile

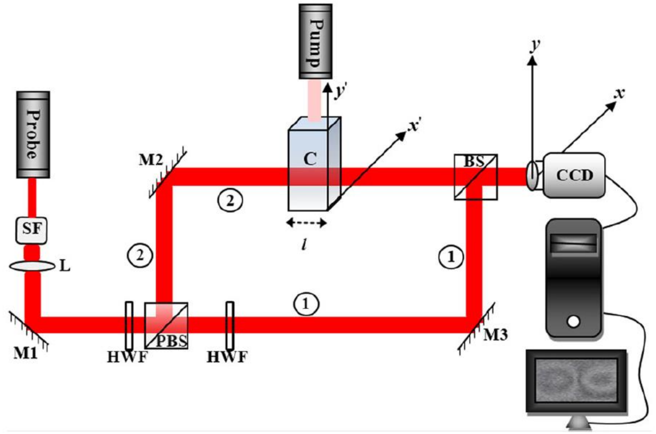


$$D = c\Delta T$$

$$D = c\left[\frac{\sqrt{5.998 - 0.644\left(b + \frac{\Delta\phi}{kl} \times 10^5\right)} - a}{0.322}\right]$$

$$\phi = \frac{D\kappa\alpha}{2c}$$

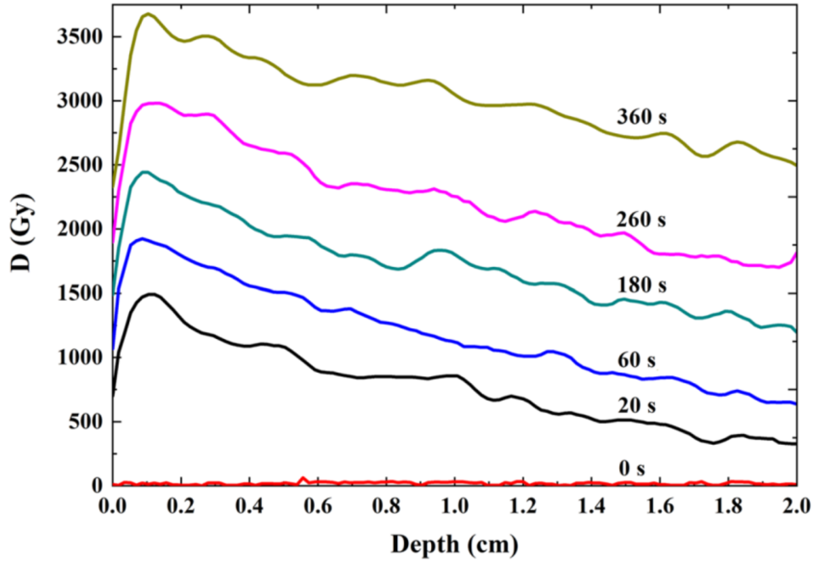


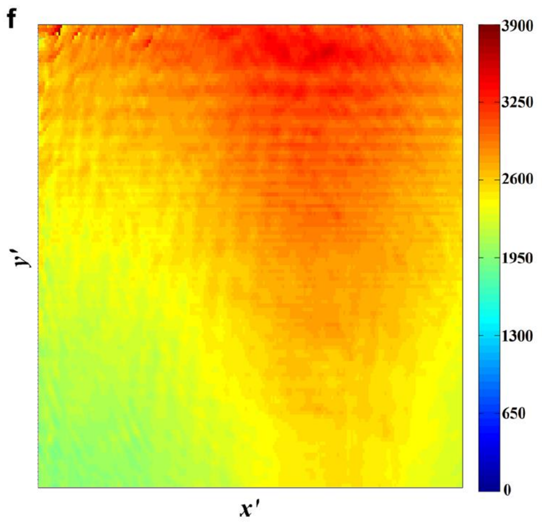


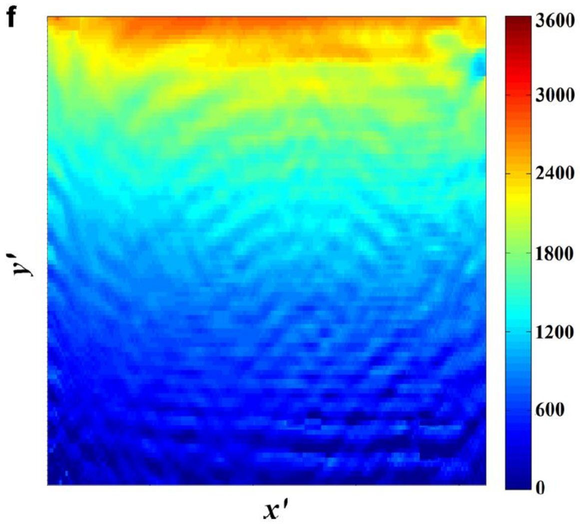


Beigzadeh AM et al A New Optical Method for Online Monitoring of the Light Dose and Dose Profile in Photodynamic Therapy. Lasers in Surgery and Medicine 52:659–670 (2020)

# Spatially Resolved Optical Properties Recovery

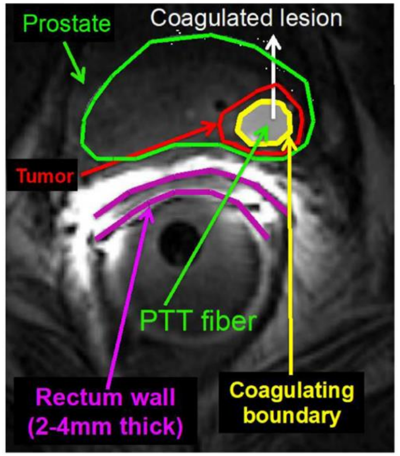


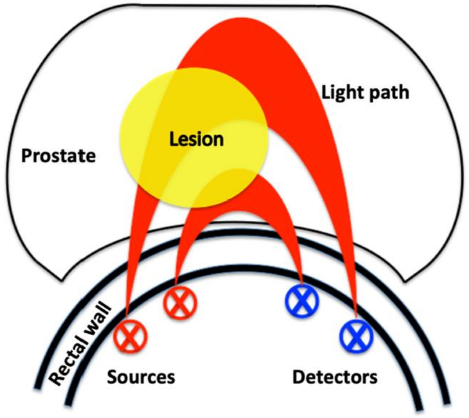


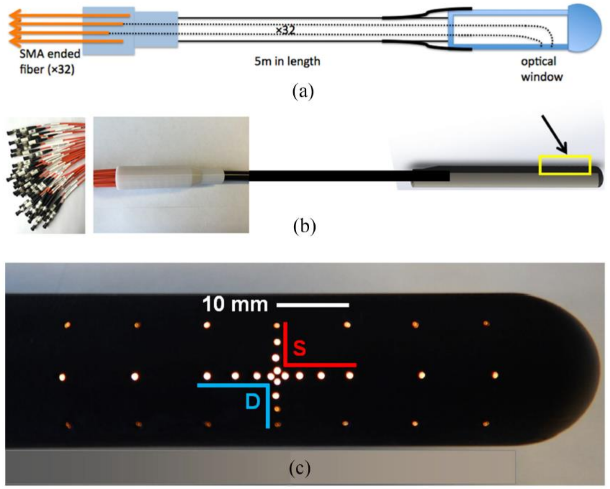


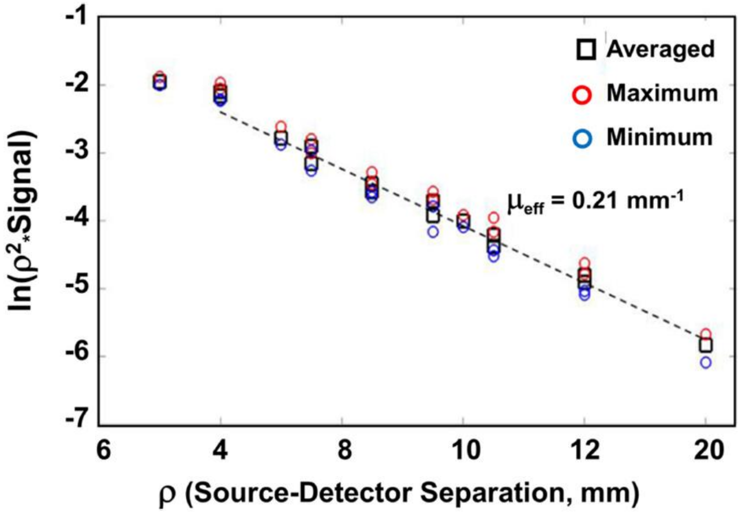


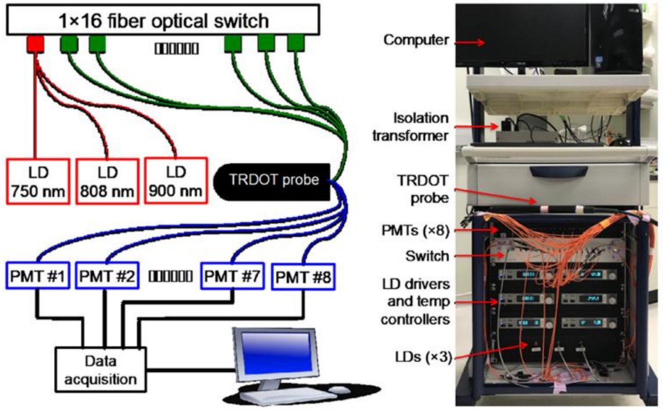


(a) (b)

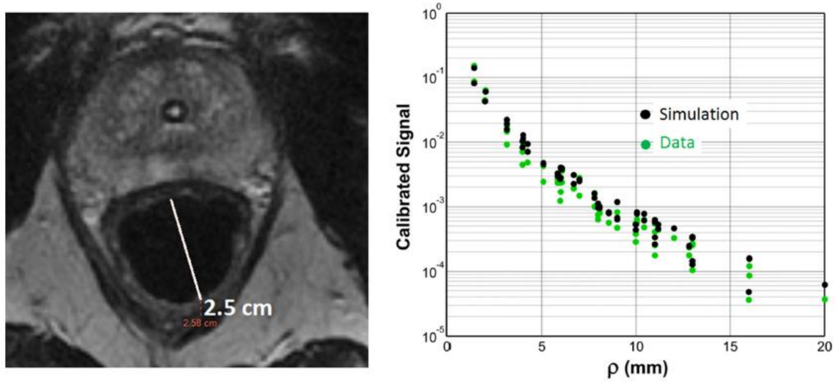


(a) (b)

He J et al. A Clinical Prototype Transrectal Diffuse Optical Tomography (TRDOT) System for *In vivo* Monitoring of Photothermal Therapy (PTT) of Focal Prostate Cancer IEEE TRANSACTIONS ON BIOMEDICAL ENGINEERING, VOL. 67, NO. 7, 2020

# Blood Volume And Flow Was Shown To Correlate With PS Uptake.

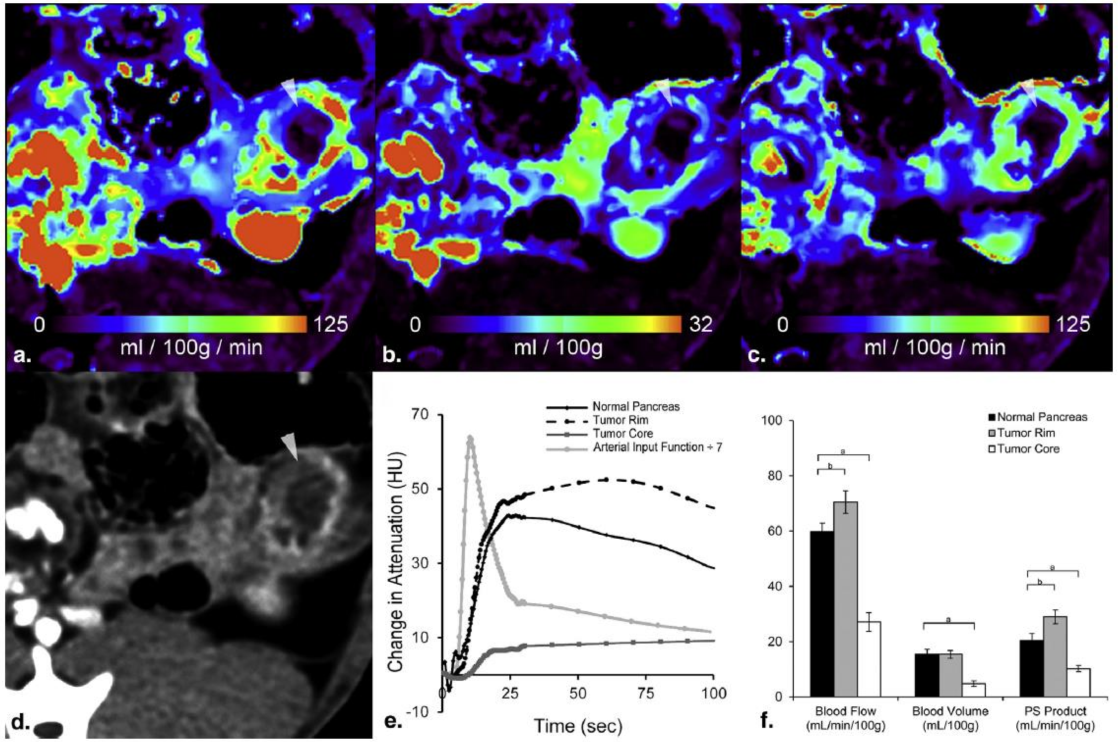


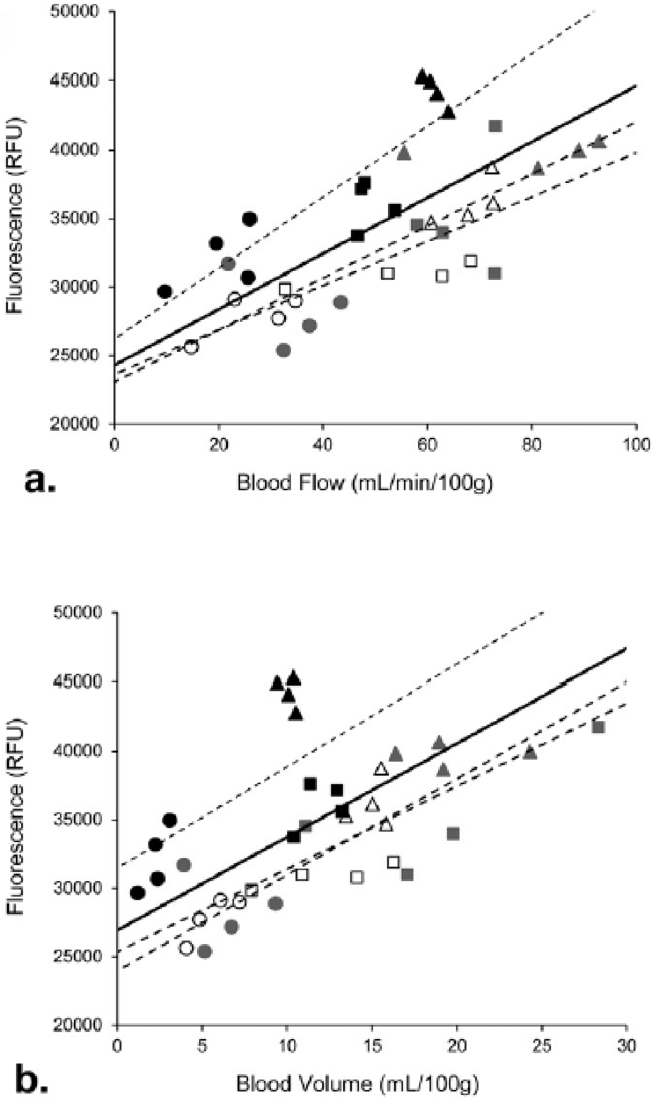


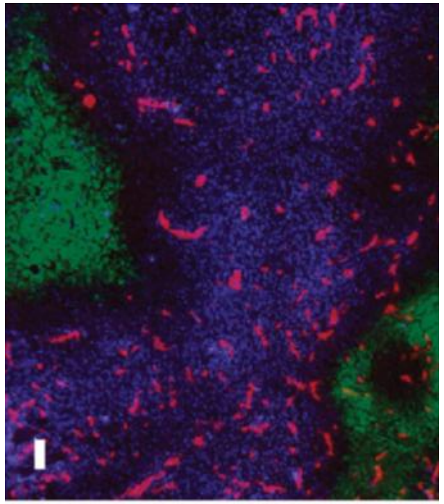

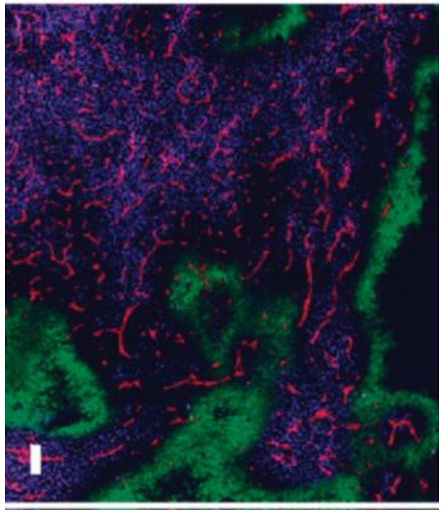

J.T. Elliott et al. Acad Radiol 2015; 22:572–579

# Tissue response to PDT

- Threshold model(s)

$$PDT_{Dose} = 2.3\varepsilon[PS]_{\lambda}\,\phi_{\lambda}(d,\mu_a,\mu_s)$$

$$PDT_{Dose} > T_{target} \qquad PDT_{Dose} < T_{host}$$

$$\frac{T_{target}}{[PS]_{target}}\frac{\phi(0)}{\phi(d)} < \frac{T_{host}}{[PS]_{host}}$$

$$\frac{T_{target}}{[PS]_{target}}\frac{\phi(r_{host})}{\phi(r_{target})} < \frac{T_{host}}{[PS]_{host}}$$

- Oxygen Consumption Model

$$\frac{d[T_1]}{dt} = BF_{ex}[PS] - \left(BF_{ex} + k_p + k_{ot}[O_2]\right)[T_1]$$

$$B = \frac{k_{isc}}{k_{isc}+k_f}\frac{\sigma}{h\nu} = \frac{\phi_t\sigma}{h\nu}$$

$$\frac{d[^3O_2]}{dt} = D_{cell}\left(\frac{1}{r^2}\frac{d}{dr}r^2\frac{d[^3O_2]}{dr}\right) - \Gamma(r,t)$$

$$\Gamma_{met} = \Gamma^0_{met}\left(\frac{[^3O_2]}{k_{met}+[^3O_2]}\right)$$

$$\Gamma_{PDT} = \Gamma^0_{PDT}\varepsilon_{PDT}\frac{[PS]}{[PS]_0}$$

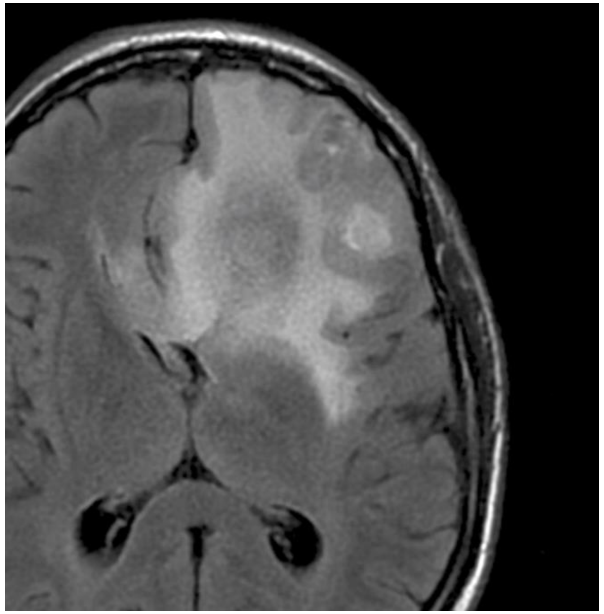

# Clinical implementation Prostate

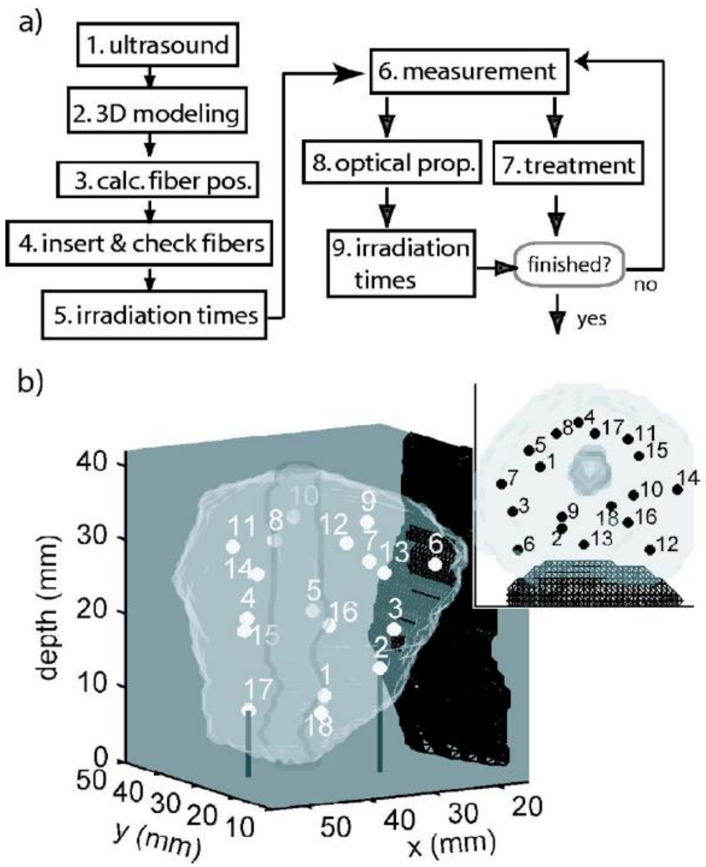



| Parameter | Prostate | Rectum | Urethra | Normal |
|---|---|---|---|---|
| $L_j$ (J) | 5 | 0 | 0 | 0 |
| $U_j$ (J) | $\infty$ | 5 | 5 | 5 |
| $\alpha_j$ | 10 | $5^a$ | 0.1 | $1e-8$ |

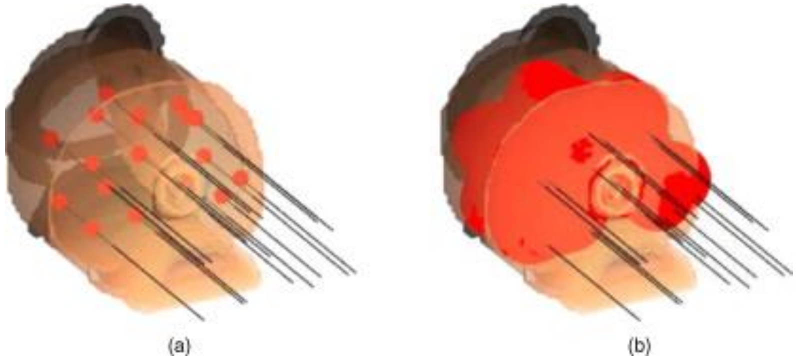


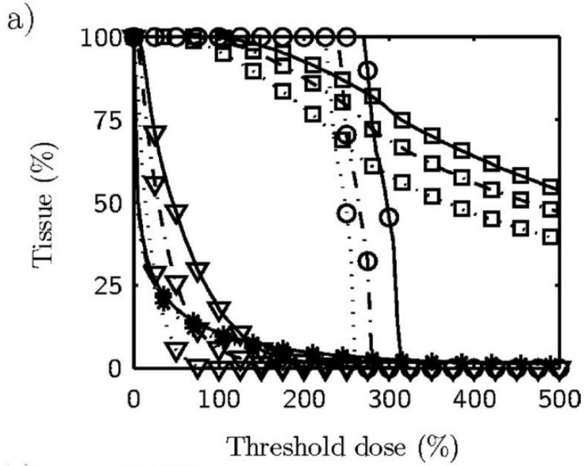


$$\phi_{ij} = \frac{P\mu_{\mathrm{eff}(i)}^2}{4\pi\mu_a|r_j - r_i|}\exp(-\mu_{\mathrm{eff}(i)}|r_j - r_i|)$$

$$\ln(\phi_{ij}|r_j - r_i|) = \ln\left(\frac{P\mu_{\mathrm{eff}(i)}^2}{4\pi\mu_a}\right) - \mu_{\mathrm{eff}(i)}|r_j - r_i|.$$

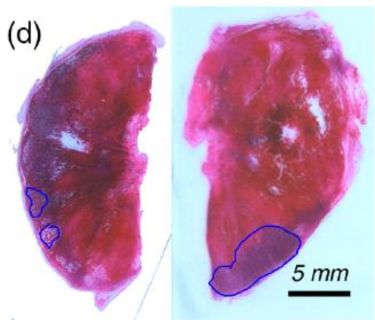


Johansson A et al Realtime light dosimetry software tools for interstitial photodynamic therapy of the human prostate. Physicists in Medicine. DOI: 10.1118/1.2790585

Johansson A et al Online dosimetry for temoporfin-mediated interstitial photodynamic therapy using the canine prostate as model Journal of Biomedical Optics 21(2), 028002

# Treatment Planning using PDT-SPACE

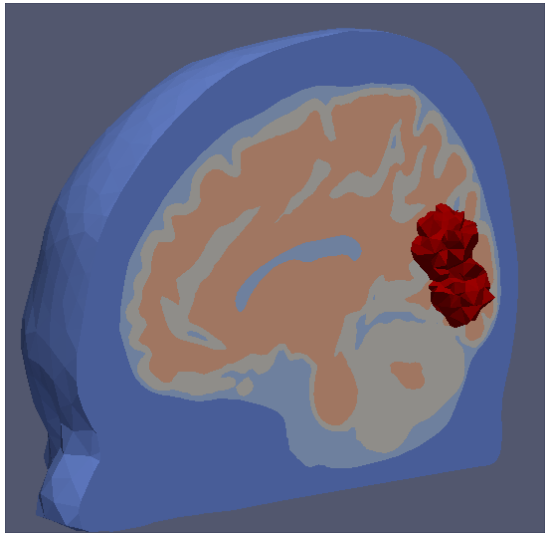

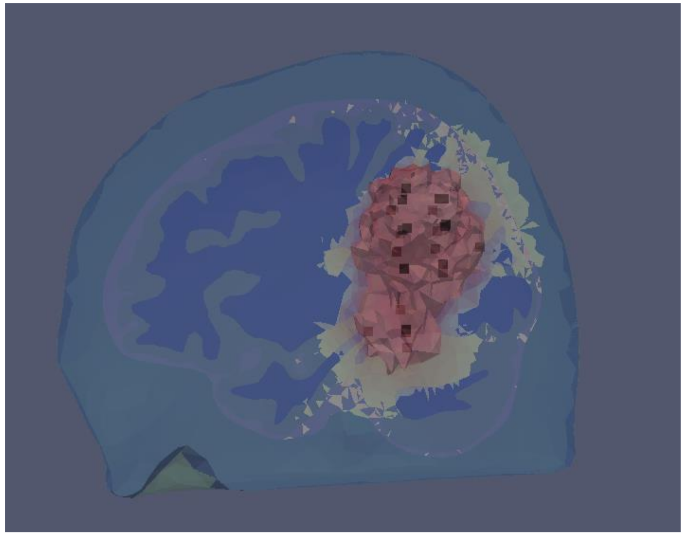

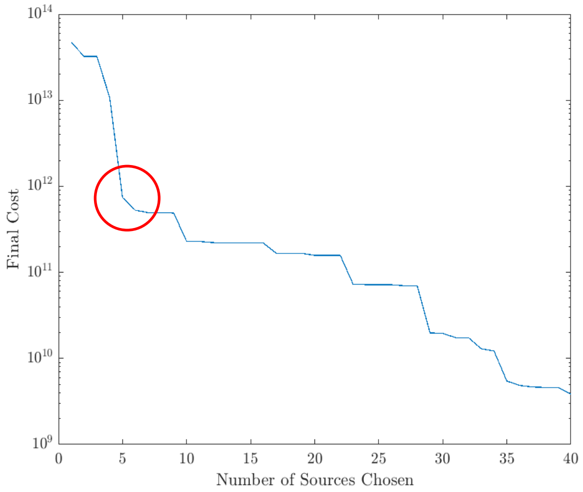


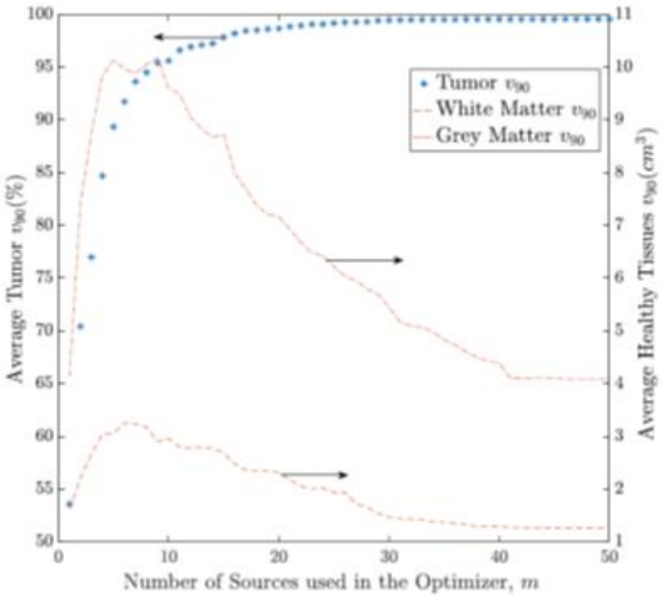


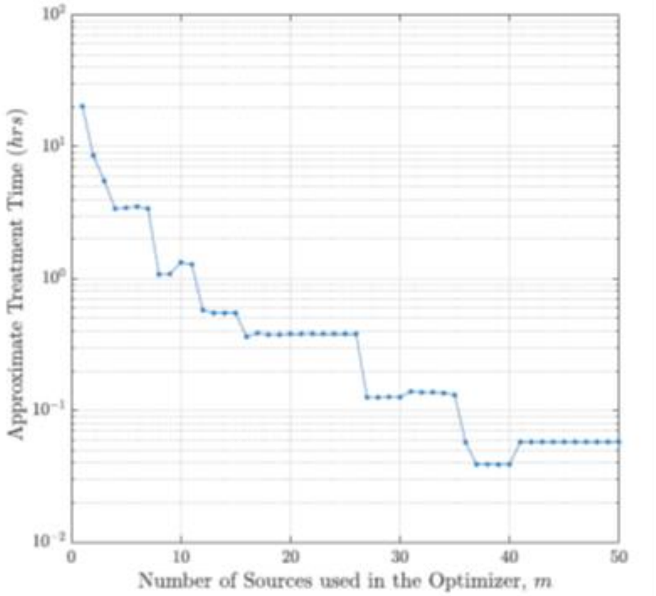


A.-A. Yassine, W. Kingsford. Y. Xu, et al. Automatic interstitial photodynamic therapy via convex optimization *Biomed. Opt. Express*, 2018

# PDT-SPACE FOR TREATMENT PLANNING

$$Dose_{PDT} = 2.3\,\varepsilon\,(\lambda)[Photosensitizer]\varphi(d)$$

Threshold Value $10^{18}$ photons/cm$^3$ absorbed

| Tissue Type | Photosensitizer | | | |
|---|---|---|---|---|
| | Photofrin | ALA | SnET | ALCIPc |
| Tumor | 18 | 1.3 | 0.6 | 28 |
| Grey Matter | 2.7 | 0.39 | 0.5 | 29 |
| White Matter | 2.8 | 14.2 | 0.01 | 42 |

| Wavelength (*nm*) | Optical Property | Tissue Type | | | | |
|---|---|---|---|---|---|---|
| | | *Tumor* | *Skull* | *CSF* | *White Matter* | *Grey Matter* |
| 630 | $\mu_a(mm^{-1})$ | 0.2 | 0.75 | 0.004 | 0.08 | 0.02 |
| | $\mu_s(mm^{-1})$ | 10 | 12.9 | 0.009 | 40.9 | 9 |
| | $g$ | 0.8 | 0.8 | 0.89 | 0.84 | 0.89 |
| | $n$ | 1.39 | 1.56 | 1.36 | 1.467 | 1.36 |

| Photosensitizer | | Photofrin | ALA | SnET | ALCIPc |
|---|---|---|---|---|---|
| Activation Wavelength (*nm*) | | 630 | 635 | 662 | 675 |
| Uptake Ratio | Tumor/Grey matter | 10.6 | 22 | 1.5 | 12.7 |
| | Tumor/White matter | 8.2 | 72 | 3.4 | 24.9 |

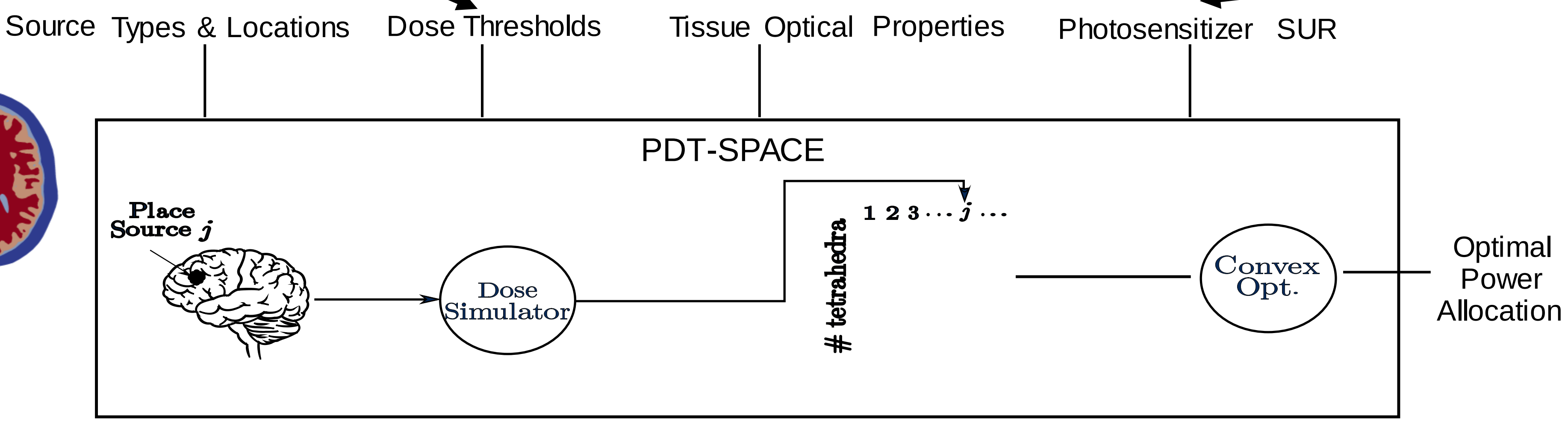


A.-A. Yassine, W. Kingsford. Y. Xu, et al. Automatic interstitial photodynamic therapy via convex optimization *Biomed. Opt. Express*, 2018

# Outcome Predictions for Spinal Metastasis

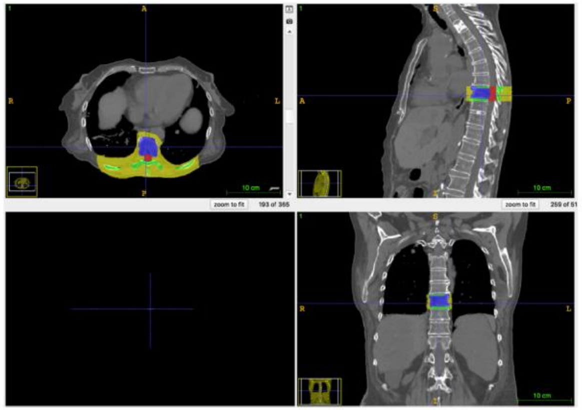

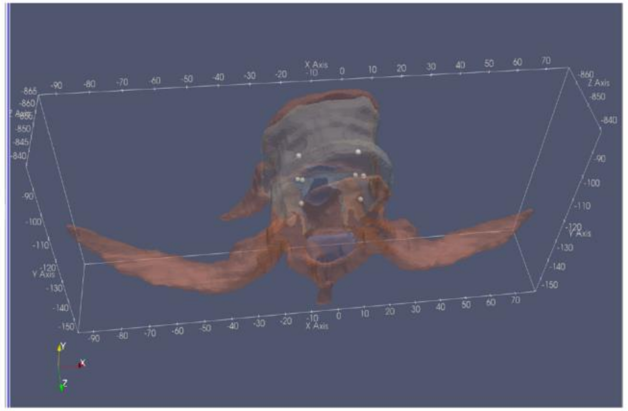

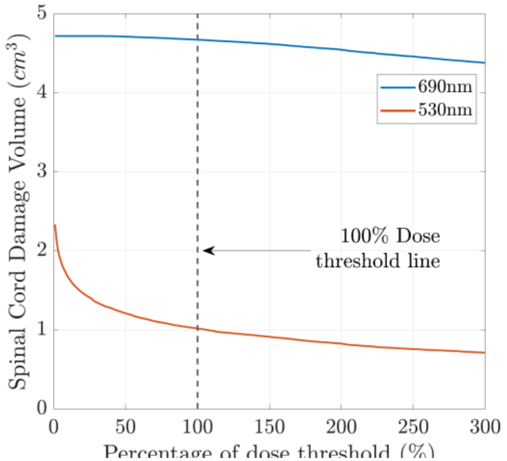


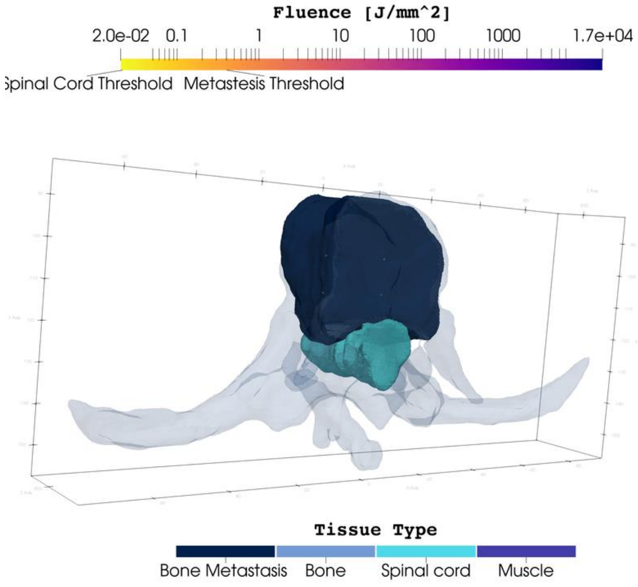


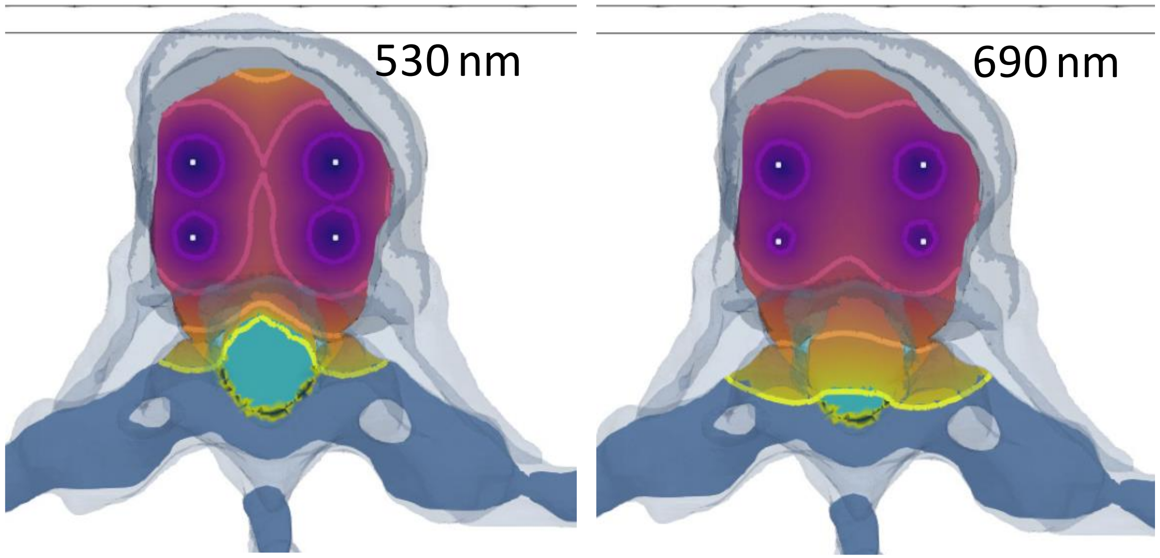


A.A. Yassine, W.C.Y. Lo, et al. Photodynamic therapy outcome modelling or patients with spinal metastasis: A simulation based study *Scientific Report (under review0*.
M. S. Patterson et al. ,In vivo tests of the concept of photodynamic threshold dose in normal rat liver photosensitized by aluminum chlorosulphonated phthalocyanine," Photochem. Photobiol. 51, 343–349 (1990)

# Approach

Heuristic:

Parallel sources.

$0.8\ cm - 1\ cm$ between every two sources.

$1\ cm$ from tumor boundary.

Simulated annealing based.

**Accurate but Slow!**

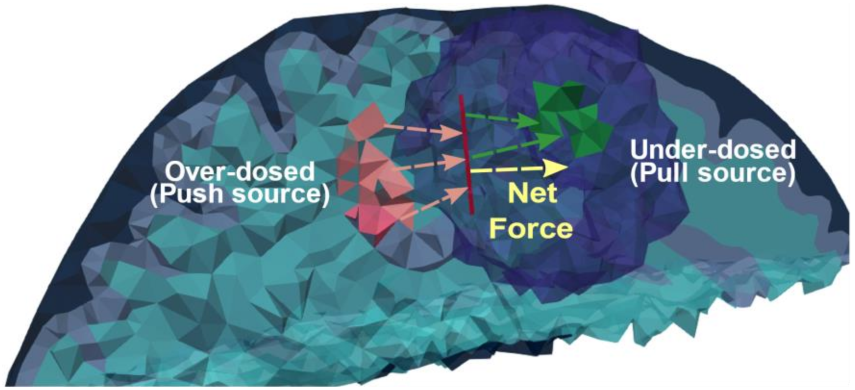


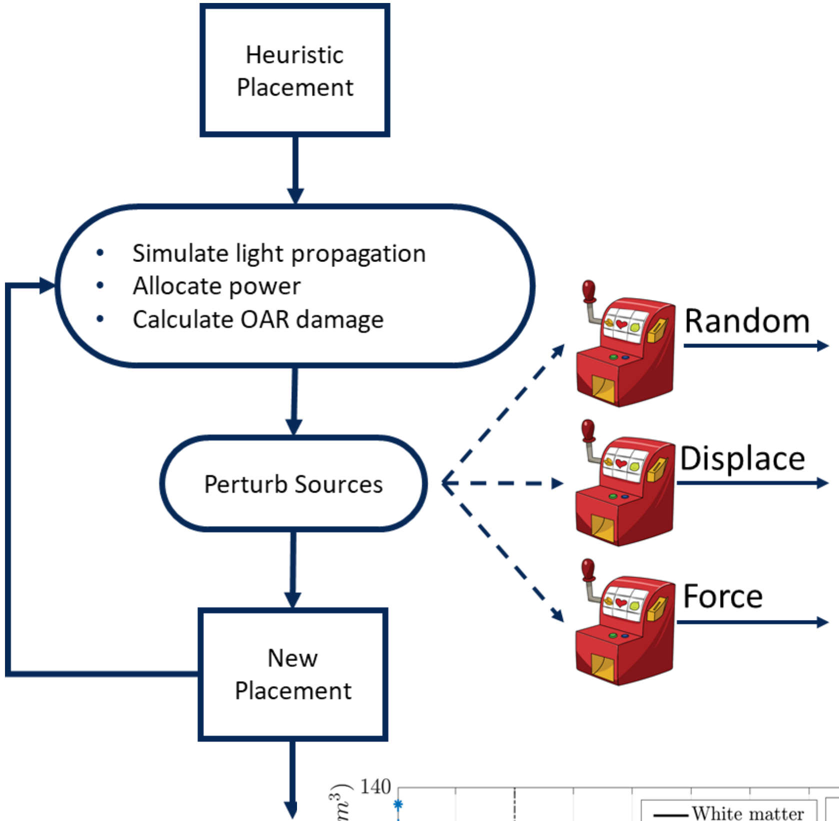


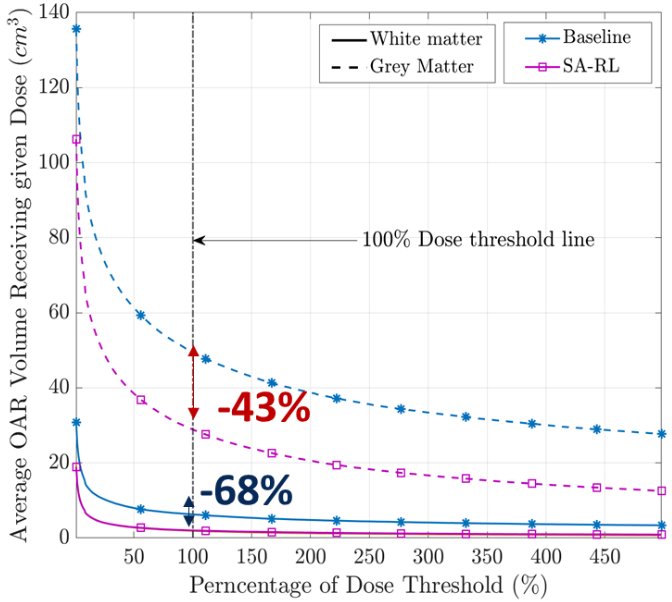


Actions:

Choose among different perturbation strategies.

Agent:

Receive reward of new perturbation.

Evaluate its effectiveness.

Select next strategy.

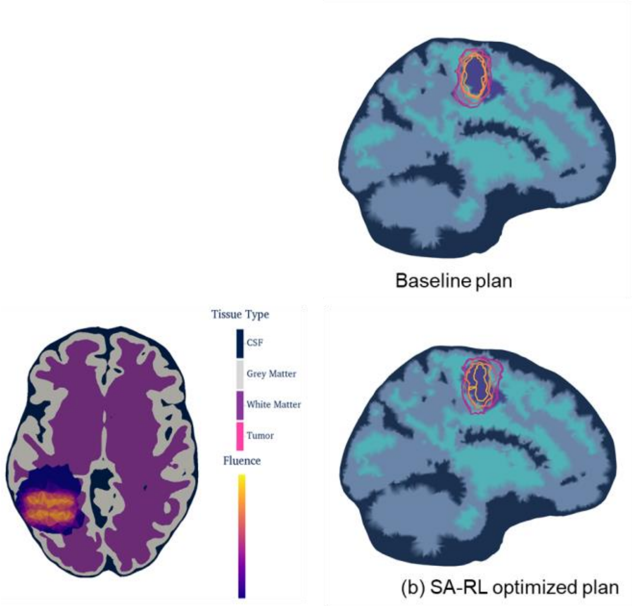

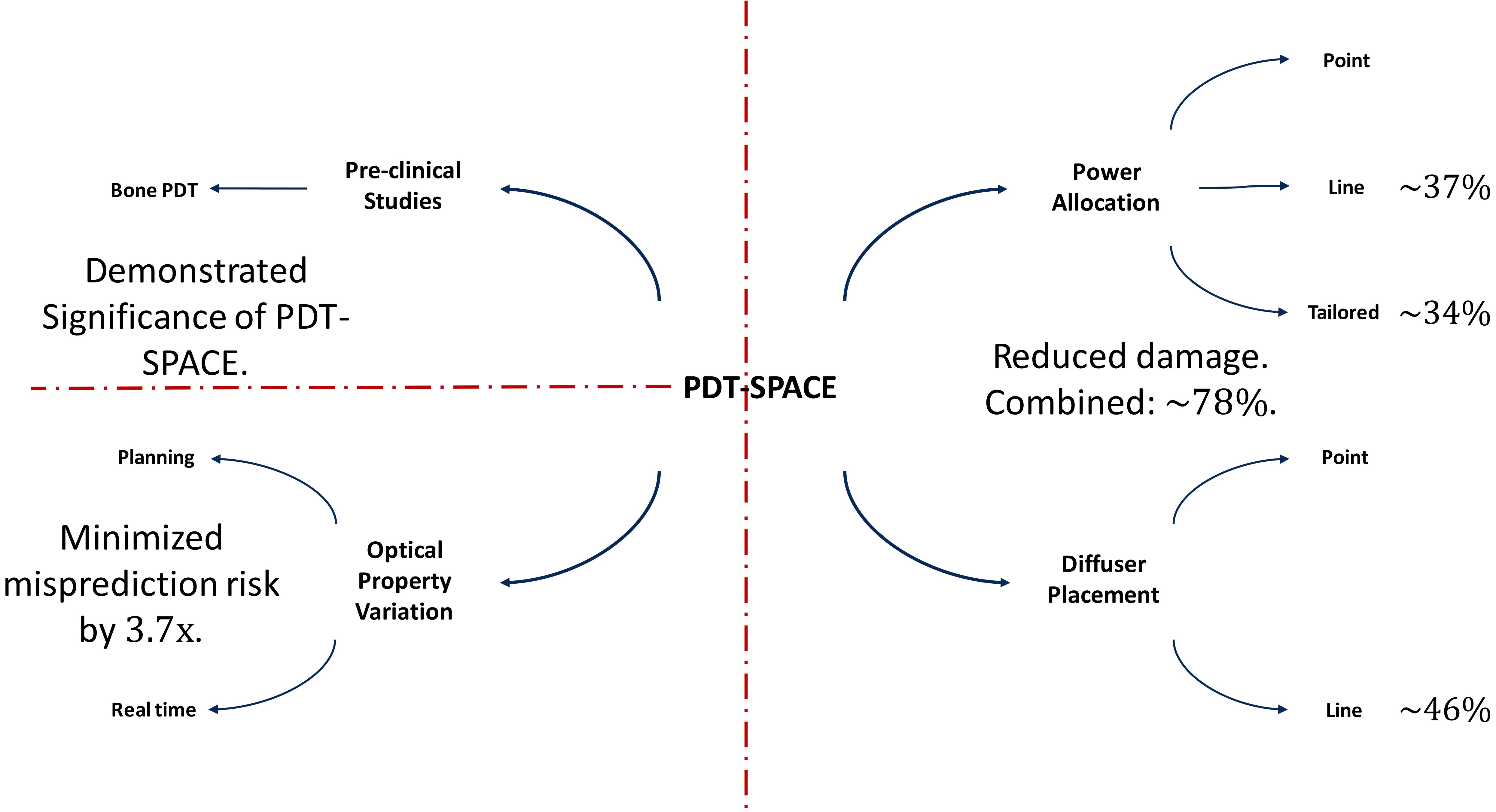
PDT-SPACE
Pre-clinical Studies
Bone PDT
Demonstrated Significance of PDT-SPACE.
Optical Property Variation
Planning
Real time
Minimized misprediction risk by 3.7x.
Power Allocation
Point
Line
~37%
Tailored
~34%
Reduced damage. Combined: ~78%.
Diffuser Placement
Point
Line
~46%

# IMPACT OF OPTICAL PROPERITES VARIATION

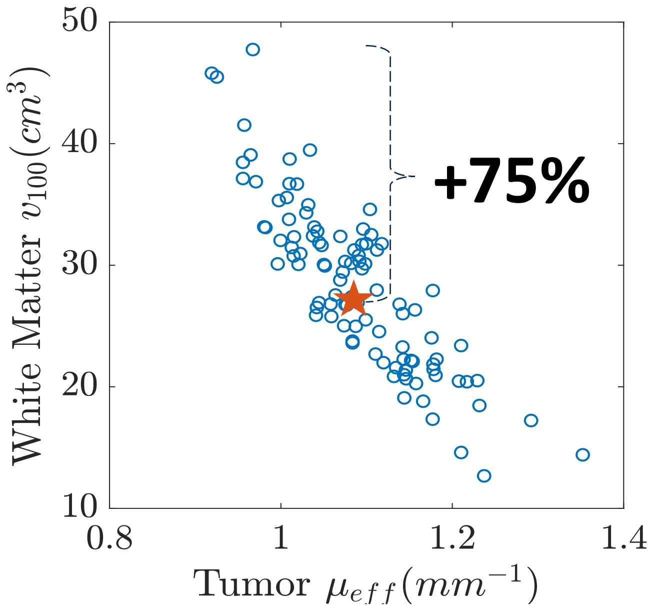


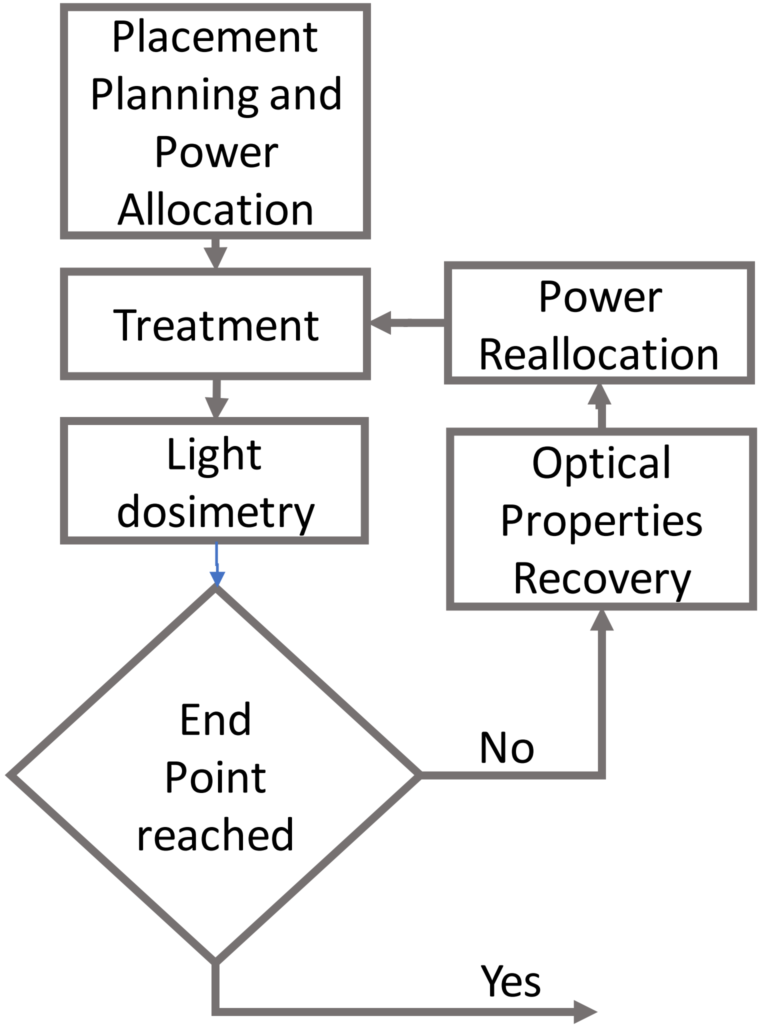


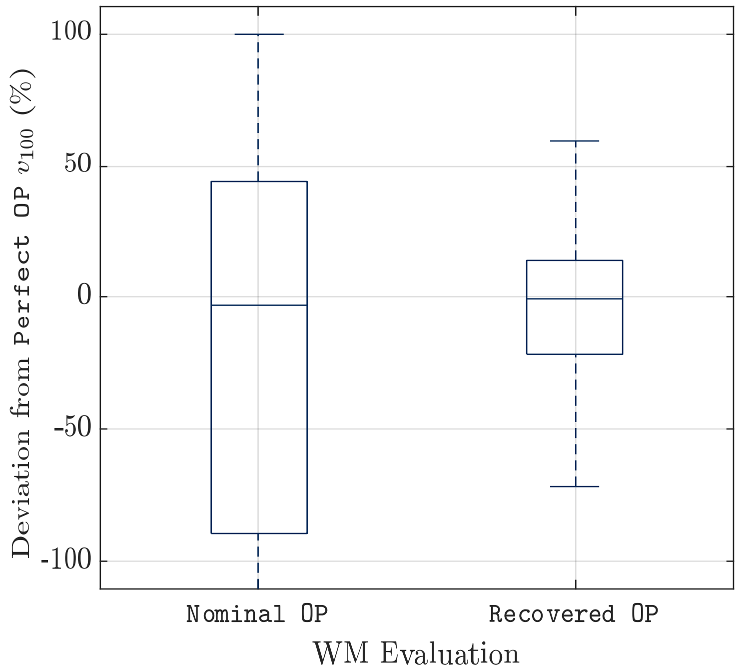


A.-A. Yassine, L. Lilge and V. Betz, “Machine learning for real-time optical property recovery in interstitial photodynamic therapy – A simulation based study,” Biomed. Opt. Express (under review)


44

# Considering ideal versus real dectors.

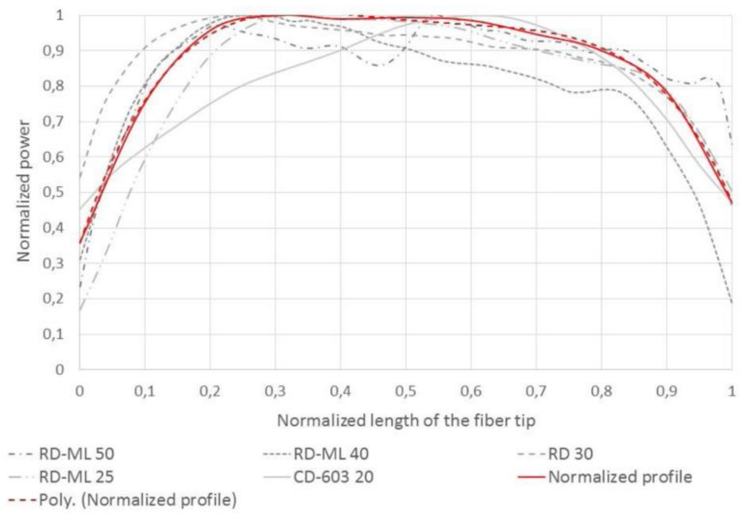


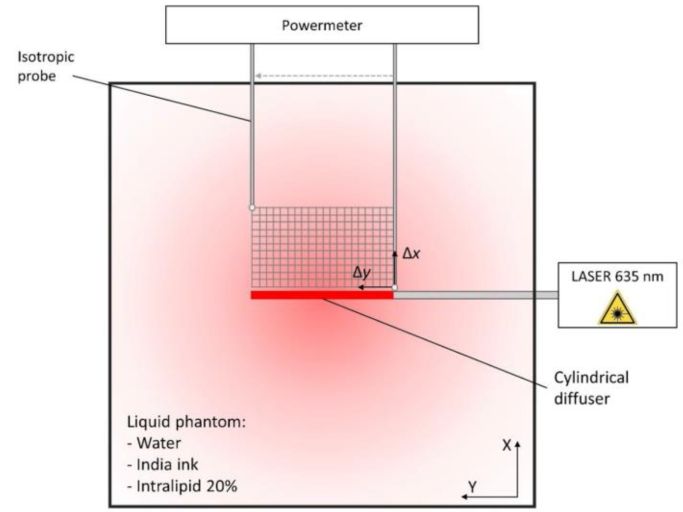


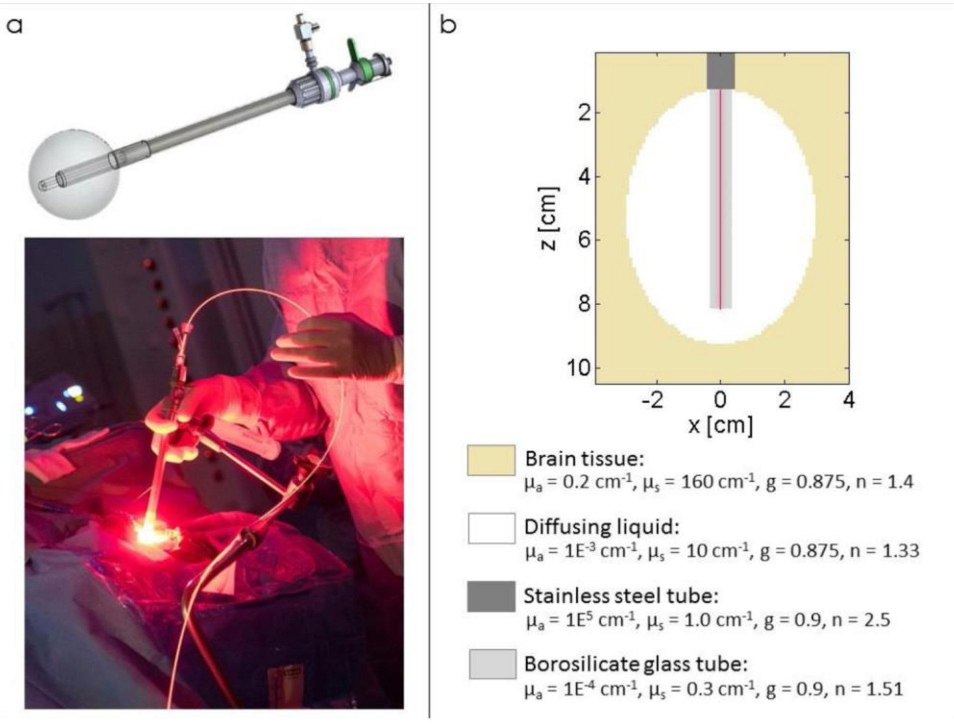


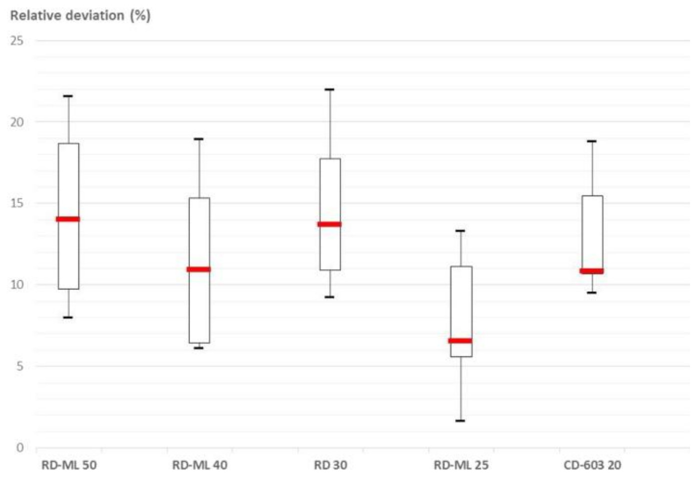


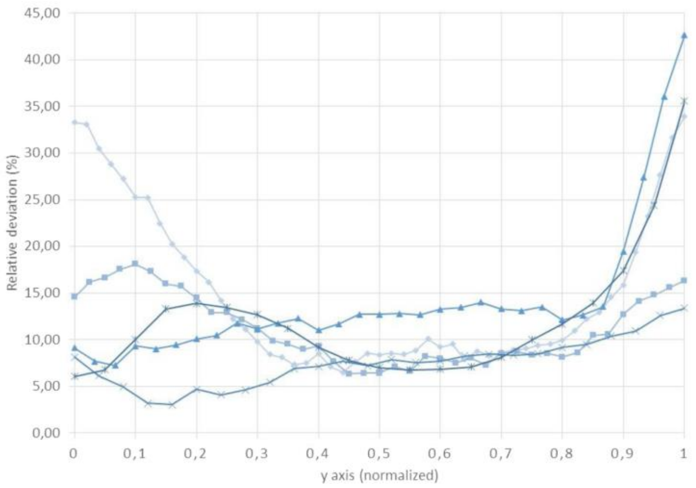


Dupont C et al. Parallelized Monte-Carlo dosimetry using graphics processing units to model cylindrical diffusers used in photodynamic therapy: From implementation to validation Photodiagnosis and Photodynamic Therapy 26 (2019) 351–360

# fMRI to adjust PDT planning input parameters

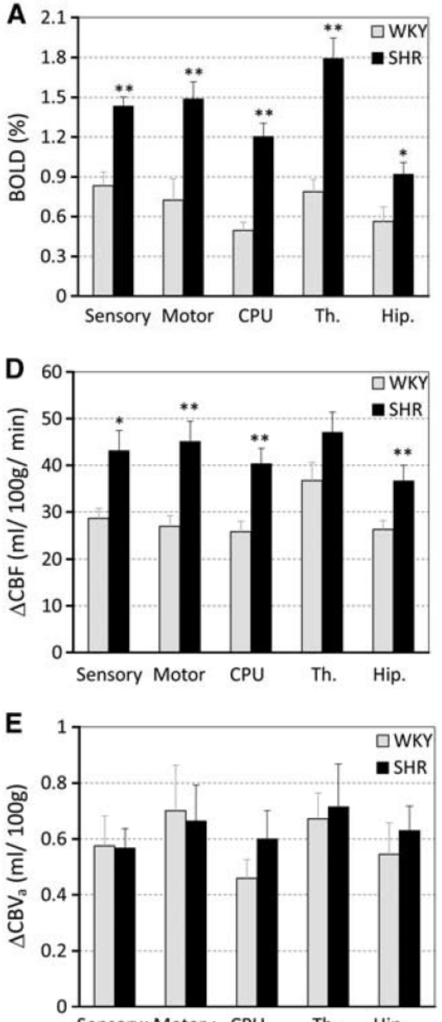


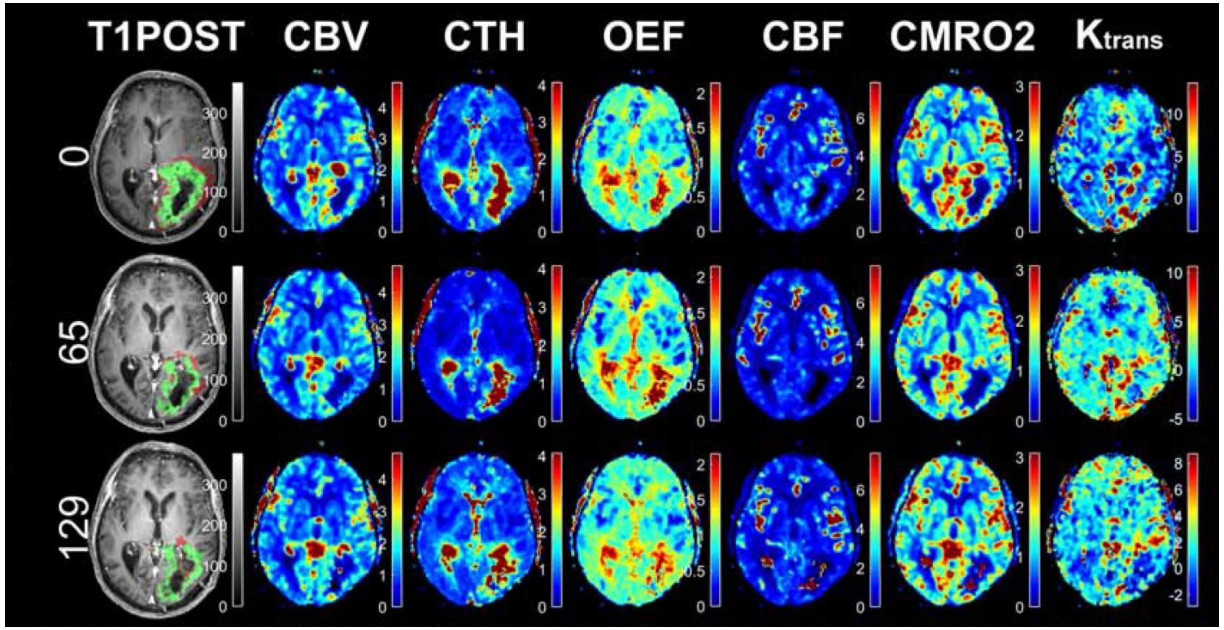


Hansen et al., *J Mag Res Img*. 2016.

CBV = cerebral blood volume
CTH = cerebral transit heterogeneity
OEF = oxygen extraction fraction
CBF = cerebral blood flow
$CMRO_2$ = metabolic rate of oxygen

$\boldsymbol{k}$ = **diffusion coefficient**

$$\alpha = \frac{-\log(2)}{\log(r) - r(\log(e)) + \log(e)}$$

$$r = \frac{t_{1/2peak} - AT}{t_{peak} - AT}$$

$$\beta = \frac{t_{peak} - AT}{\alpha}$$

$Q$ = capillary extraction fraction

Diffusion Coefficient from OEF: $\int_0^\infty \frac{1}{(\boldsymbol{k}\beta)^\alpha \Gamma(\alpha)} \tau^{\alpha-1} e^{\frac{-\tau}{\boldsymbol{k}\beta}} Q(\tau)\, d\tau$

**Hansen, et al., (2016). Reliable Estimation of Microvascular Flow Patterns in Patients with Disrupted Blood-Brain Barrier Using Dynamic Susceptibility Contrast MRI. Journal of Magnetic Resonance.**

# Summary

- Precision iPDT using Anatomical detail is realized.
- Monitoring for personalize tissue optical properties required
  - Possibly under sampled by sensors
  - Need to employ clinical functional Imaging for heterogenous
- Predicting local $pO_2$ is possible using fMRI resolution
  - k for oxygen has been determined
- Predicting local PS distribution might be possible based on Blood Flow and Blood Volume
  - Needs to determine the bi-directional extravasation coefficient, k, of each photosensitizer
- Most importantly one needs to know the tissue response

# Standardized reporting of PDT response

ALA induced PpIX mediated PDT in vitro

| Cell Line | λ [nm] | $LD_{50}$ [μM] ALA | $T_{LD50}$ [hν cm$^{-3}$] |
|---|---|---|---|
| HeLa | 540 | 2.1 | $7.8\ 10^{16}$ |
| RPE-1 | 540 | 3.3 | $1.2\ 10^{17}$ |
| HeLa | 600-700 | 3.1 | $1.2\ 10^{17}$ |
| SiHa | 600-700 | 6.25 | $2.4\ 10^{17}$ |
| MDA-MB-23 1 | 600-700 | 3.5 | $1.3\ 10^{17}$ |
| 2780AD | 600-700 | 4.8 | $1.8\ 10^{17}$ |
| A2780-9S | 600-700 | 3.5 | $1.3\ 10^{17}$ |

TLD1433 mediated PDT in vitro

| Cell LIne | λ [nm] | $LD_{50}$ [μM] | $T_{LD50}$ [hν cm$^{-3}$] |
|---|---|---|---|
| Skmel28 | 625 | 2.29 | $8.7\ 10^{16}$ |
| HL-60 | 625 | 7.7 | $2.9\ 10^{17}$ |
| CT26 | 525 | 0.021 | $9.8\ 10^{15}$ |
| CT26.CL25 | 525 | 0.011 | $5.2\ 10^{15}$ |
| U87 | 525 | 0.051 | $2.4\ 10^{16}$ |
| F98 | 525 ± 25 | 2.81 | $1.3\ 10^{17}$ |
| T24 | 525 ± 25 | 0.0077 | $1.5\ 10^{15}$ |
| AY27 | 525 ± 25 | 0.0039 | $7.7\ 10^{14}$ |
| A549 | 532 | 0.099 | $1.6\ 10^{16}$ |
| RG-2 | 530 | 0.0265 | $2.4\ 10^{16}$ |

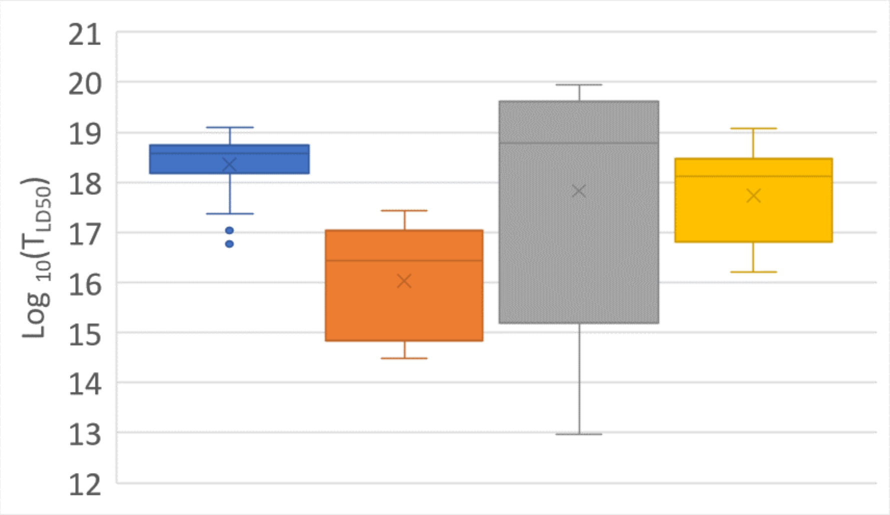

# FullMonte

Fast Tetrahedral based photon propagation simulator
Open-source, rich set of input, output, and analysis tools
Robust framework for statistical verification
Data formats shared with class-leading visualization tools (.vtk)
Reads and write file formats from other similar simulators, (TIM-OS, MMC, COMSOL (finite-element simulations), and MCML)
Platform Linux, Windows and Mac IO

## Your Infrastructure

Docker images for SW

Https://gitlab.com/FullMonte/FullMonteSW

CUDAAccel

https://gitlab.com/FullMonte/cudaaccel

MeshTool

https://gitlab.com/FullMonte/MeshTool

PDT-SPACE

https://gitlab.com/FullMonte/pdt-space

## Cloud (AWS)

FullMonteWEB

Http://fullmontesuite.herokuapp.com/application/

Access to GPU version

Access to PDT-SPACE

T Young-Schultz, S Brown, et al. FullMonteCUDA: GPU-accelerated Monte Carlo Simulator for Light Propagation BOE 10 (9) 4711-4726 (2019)
A.-A. Yassine, W. Kingsford, et al. Automatic interstitial photodynamic therapy via convex optimization Biomed. Opt. Express, 2018.
J Cassidy, S Lia et al. FullMonte high-performance, customizable Monte Carlo biophotonic simulator" JBO (2018)